

HyperFast: Instant Classification for Tabular Data

David Bonet^{1,2}, Daniel Mas Montserrat¹, Xavier Giró-i-Nieto^{3*}, Alexander G. Ioannidis¹

¹Stanford University, Stanford, CA, USA

²Universitat Politècnica de Catalunya, Barcelona, Spain

³Amazon, Barcelona, Spain
ioannidis@stanford.edu

Abstract

Training deep learning models and performing hyperparameter tuning can be computationally demanding and time-consuming. Meanwhile, traditional machine learning methods like gradient-boosting algorithms remain the preferred choice for most tabular data applications, while neural network alternatives require extensive hyperparameter tuning or work only in toy datasets under limited settings. In this paper, we introduce HyperFast, a meta-trained hypernetwork designed for instant classification of tabular data in a single forward pass. HyperFast generates a task-specific neural network tailored to an unseen dataset that can be directly used for classification inference, removing the need for training a model. We report extensive experiments with OpenML and genomic data, comparing HyperFast to competing tabular data neural networks, traditional ML methods, AutoML systems, and boosting machines. HyperFast shows highly competitive results, while being significantly faster. Additionally, our approach demonstrates robust adaptability across a variety of classification tasks with little to no fine-tuning, positioning HyperFast as a strong solution for numerous applications and rapid model deployment. HyperFast introduces a promising paradigm for fast classification, with the potential to substantially decrease the computational burden of deep learning. Our code, which offers a scikit-learn-like interface, along with the trained HyperFast model, can be found at <https://github.com/AI-sandbox/HyperFast>.

Introduction

Many different machine learning (ML) methods have been proposed for the task of supervised classification (Duda, Hart, and Stork 2000), following a traditional two-stage methodology. The initial stage involves the optimization of a model using the training portion of a dataset. Several tuning iterations are performed with the aim of finding the hyperparameter configuration of the model that yields the best performance on the specific task. In the second stage, the model with the chosen hyperparameter setup is used for evaluation and inference on the test set. Training and tuning models for classification tasks is time-consuming, and it often requires extensive data pre-processing, expertise in selecting hyperparameters that could fit the task at hand, and a validation

process. Further, the computational and temporal costs of the traditional process can be prohibitive, particularly in real-time and large-scale applications, such as healthcare (Esteva et al. 2019), or applications where rapid model deployment is necessary (Deiana et al. 2022), including data streaming, where models need to be updated or re-trained frequently. In this work, we propose HyperFast, a novel method to solve classification tasks from multiple domains with a single forward pass of a hypernetwork. We substitute the slow training stage of a classification network with a fixed hypernetwork that has been pre-trained (meta-trained) to predict the weights of a smaller neural network (i.e. main network) that can instantly solve the classification task with state-of-the-art performance. Recently, TabPFN (Hollmann et al. 2023) has been proposed, introducing a pre-trained Transformer that is able to perform classification without training. However, it is constrained to ≤ 1000 training examples, 100 features and 10 classes, which limits its application to most real-world scenarios. In this study, we are particularly interested in ensuring adaptability to large dataset sizes, filling the gap present in the current landscape of pre-trained models for instant tabular data classification. Our model is designed to work with both large and small datasets, while also providing adaptability to different numbers of samples, features, and categories.

During the meta-training stage, the hypernetwork parameters are learnt and the parameters of a main model are inferred, that is, we are “learning to learn” from a wide variety of datasets (meta-training datasets) from different modalities for which HyperFast generates a smaller neural model that performs the actual classification. During the meta-testing or inference stage, HyperFast receives a “support set” of an unseen dataset (both features and labels), and predicts a set of weights for the main model, which classifies the test samples of the dataset. In this way, the process of adapting the model to a new dataset is accelerated, and the model that does the meta-learning is decoupled from the model that does the actual inference on the data. In other words, we train a high-capacity meta-model to encode task-specific characteristics in the weights of a smaller model. Model size is also decoupled, which means that a large meta-learner can be trained just once, while many lightweight models generated by the meta-learner can be used for deployment in different applications such as edge computing, IoT devices, and mo-

*Work done prior to joining Amazon.

ble devices, where computational resources are constrained, and fast inference is indispensable. These properties are also helpful to accelerate production, improve privacy aspects, or for federated learning (Yang et al. 2019). The meta-learner can instantly generate a model that is ready for deployment, but the generated weights might not be optimal. Thus, we also explore further improvements to quickly boost the performance before deployment and leverage all the power of the framework. For example, ensembles of multiple generated models can be used, or the generated weights can be used as an initial point for fine-tuning. More detail on many of the possibilities to improve model performance and obtain a stronger predictor can be found in the Appendix.

The hypernetwork is trained on a wide range of datasets with different data distributions, allowing it to learn relevant and general meta-features, such that during testing the hypernetwork can adapt and predict an accurate set of weights for new unseen datasets. We evaluate the performance of HyperFast across a set of 15 tabular datasets, including genomics datasets and a standardized suite of datasets from OpenML (Bischl et al. 2021). We also analyze the performance of HyperFast on larger time budgets by ensembling main networks generated with multiple forward passes and fine-tuning on inference. We compare our model to similar approaches and classical methods, both in terms of performance and time. Our method achieves competitive results compared to standard ML and AutoML algorithms tuned for up to one hour for each test dataset.

Related Work

Hypernetworks. Building from evolutionary algorithms, HyperNEAT (Stanley, D’Ambrosio, and Gauci 2009) evolves Compositional Pattern-Producing Networks (CPPNs) to augment the weight structure for a larger main network. Based on this idea, (Ha, Dai, and Le 2017) propose hypernetworks, where one neural network is used to generate weights for another neural network. The hypernetwork is trained end-to-end jointly with the main network to solve the task, producing weights in a deterministic way. (Krueger et al. 2018) and (Louizos and Welling 2017) propose variational approximations for weight generation using normalizing flows, (Deutsch 2018) use multilayer perceptrons (MLPs) and convolutions, and (Ratzlaff and Fuxin 2019) use generative adversarial networks (GANs). (Schürholt et al. 2022) explores unsupervised weight generation through model datasets. (Ashkenazi et al. 2022) use neural representations similar to NeRF (Mildenhall et al. 2020) to reconstruct weights of a pre-trained network leveraging knowledge distillation. The HyperTransformer (Zhmoginov, Sandler, and Vladymyrov 2022) is a few-shot learning hypernetwork based on the Transformer architecture that generates weights of a convolutional neural network (CNN). Unlike our method, the HyperTransformer is only designed for image classification and also requires training image and activation feature extractors. HyperFast presents a novel approach by introducing hypernetworks for instant tabular classification. HyperFast solves the classification task by taking a set of labeled datapoints (support set) and generating the weights of a neural model that can

be directly used to classify new unseen datapoints. Previous work (Gidaris and Komodakis 2018; Qiao et al. 2018) considered generating weights for specific layers (e.g., the last classification layer), while training the rest of the feature extractor. Here, we go one step further and consider generating all the weights of the model that performs the classification in a single forward pass. Our hypernetwork design includes initial transformation modules, retrieval-based components, and different pooling operations in a unique architecture, offering feature permutation invariance and providing scalability and adaptability to new datasets while ensuring efficiency and speed.

Meta-learning. In the context of rapidly adapting to new tasks using limited data, meta-learning methods have emerged as powerful techniques. These approaches “learn to learn” by quickly integrating information at test time to make predictions for new, unseen tasks. A model $P_\theta(y|x, \mathcal{S})$ is learned for every new task, where y is the target, x is the test input, and $\mathcal{S} = \{X, Y\}$, is the support set. Metric-based learning methods such as Matching Networks (Vinyals et al. 2016) and Prototypical Networks (Snell, Swersky, and Zemel 2017) map a labelled support set \mathcal{S} into an embedding space, where a distance is computed with the embedding of an unlabelled query sample to map it to its label. As in kernel-based methods, the model P_θ can be obtained through $P_\theta(y|x, \mathcal{S}) = \sum_{x_i, y_i \in \mathcal{S}} K_\theta(x, x_i) y_i$. Optimization-based methods such as Model-agnostic meta-learning (MAML) (Finn, Abbeel, and Levine 2017) learn an initial set of model parameters and perform an additional optimization through a function $f_{\theta(\mathcal{S})}$, where model weights θ are adjusted with one or more gradient updates given the support set of the task \mathcal{S} , i.e., $P_\theta(y|x, \mathcal{S}) = f_{\theta(\mathcal{S})}(x, \mathcal{S})$. Finally, model-based approaches such as Neural Processes (NPs) (Garnelo et al. 2018b,a) first process both support samples and query samples independently as in Deep Sets (Zaheer et al. 2017), and the predicted embeddings are aggregated with a permutation-invariant pooling operation, resulting in a dataset-level summary that is fed to a second stage network that predicts the output for the query sample. The overall model is defined by a function f and the process can be mathematically described as $P_\theta(y|x, \mathcal{S}) = f_\theta(x, \mathcal{S})$. Similarly, TabPFN (Hollmann et al. 2023) learns to learn Bayesian inference by using a Transformer network. In contrast, our method directly obtains the model weights θ in a single forward step through an independent network, i.e., the hypernetwork h , such that $P_\theta(y|x, \mathcal{S}) = f_{h(\mathcal{S})}(x)$.

Deep Learning for Tabular Data. Although deep learning (DL) models achieve state-of-the-art results in many domains (e.g., language, computer vision, audio), this is not the case for tabular data. Tree-based models such as XGBoost (Chen and Guestrin 2016), LightGBM (Ke et al. 2017) or CatBoost (Prokhorenkova et al. 2018) are still the preferred choice in some tabular data applications (Grinsztajn, Oyalon, and Varoquaux 2022; Shwartz-Ziv and Armon 2022). AutoML methods (He, Zhao, and Chu 2021; Feuerer et al. 2020; Erickson et al. 2020) are also a popular alternative, automatically selecting the most appropriate ML algorithm and its hyperparameter configuration. However, it has been

shown that there is not a universal superior solution (Gorishniy et al. 2021; McElfresh et al. 2023), and many deep learning approaches for tabular data have been proposed (Kadra et al. 2021; Arik and Pfister 2021; Somepalli et al. 2021; Kossen et al. 2021; Gorishniy et al. 2021; Yan et al. 2023; Chen et al. 2022a; Katzir, Elidan, and El-Yaniv 2020; Popov, Morozov, and Babenko 2019; Hollmann et al. 2023; Chen et al. 2022b, 2023; Zhu et al. 2023; Zhang et al. 2023). (Kadra et al. 2021) introduced Regularization Cocktails, where different regularization techniques are applied to simple MLPs to boost performance. Recent work has explored using attention mechanisms to improve performance on tabular data. TabNet (Arik and Pfister 2021) adopts sequential attention on subsets of features, SAINT (Somepalli et al. 2021) applies attention over rows and columns in a BERT-style fashion and uses contrastive pre-training with data augmentation, NPT (Kossen et al. 2021) introduces attention between data points, ExcelFormer (Chen et al. 2023) models feature interaction and feature representation alternately, FT-Transformer (Gorishniy et al. 2021) adapts a Transformer with embeddings for categorical and numerical features, and T2G-Former (Yan et al. 2023) includes a graph estimator to guide tabular feature interaction. TabCaps explore capsule networks (Chen et al. 2022a), Net-DNF (Katzir, Elidan, and El-Yaniv 2020) disjunctive normal formulas, NODE (Popov, Morozov, and Babenko 2019) combines ensembles of differential oblivious decision trees with multi-layer hierarchical representations, DANets (Chen et al. 2022b) learn groups of correlative input features to generate higher-level features, and other works explore large language models (LLM) for tabular data pre-training (Zhu et al. 2023; Zhang et al. 2023). Nevertheless, most of the proposed DL models for tabular data require slow training and custom hyperparameter tuning for every new dataset. In contrast, we focus on off-the-shelf models that do not need extensive tuning for a new task. In this direction, TabPFN (Hollmann et al. 2023) pre-trains a Transformer on synthetic data given a prior to perform tabular data classification in a single forward pass with no hyperparameter tuning. However, TabPFN can only be applied to small tabular datasets, i.e., ≤ 1000 training examples, 100 features and 10 classes.

Background

Meta-Learning Problem Setting

In our meta-learning experiments, we train a model h (i.e., the hypernetwork) that is able to quickly adapt to new tasks given some observations, and generate the weights of a main model f that solves the task for unseen datapoints. We consider a set of classification tasks \mathcal{T} where each task $t \in \mathcal{T}$ is associated with a *support set* \mathcal{S}_t of examples that are sufficient to find the optimal model f that solves the task, a loss function \mathcal{L}_t , and a *query set* \mathcal{Q}_t to define \mathcal{L}_t . The first phase is the *meta-training*, where in each step a different training task $t \in \mathcal{T}_{\text{meta-train}}$ is selected. We compile a set of meta-training datasets $\mathcal{D}_{\text{meta-train}}$, where each dataset $d \in \mathcal{D}_{\text{meta-train}}$ is composed of a training set d_{train} and a test set d_{test} , as in the common machine learning setup. In each meta-training step, a task $t \in \mathcal{T}_{\text{meta-train}}$ is sampled by first randomly choosing

a meta-training dataset d . Then, \mathcal{S}_t and \mathcal{Q}_t are generated by sampling examples from d_{train} and d_{test} , respectively. Meta-validation is also performed intermittently through meta-training, where a separate set of meta-validation datasets $\mathcal{D}_{\text{meta-val}}$ is used to generate validation tasks $\mathcal{T}_{\text{meta-val}}$ to evaluate our algorithm and select the best performing model.

Once HyperFast is trained, an independent set of meta-testing datasets $\mathcal{D}_{\text{meta-test}}$ are used to create the evaluation tasks $\mathcal{T}_{\text{meta-test}}$ in which the selected model is evaluated. This approach allows us to extend the classical “ n -way- k -shot” few-shot learning setting to handle multiple datasets with varying distributions and categories, testing the robustness and generalization of our model on new data.

As opposed to the training tasks, where each $t \in \mathcal{T}_{\text{meta-train}}$ is randomly generated at every meta-training step, $\mathcal{T}_{\text{meta-val}}$ and $\mathcal{T}_{\text{meta-test}}$ are sets of partially fixed tasks, as the query set \mathcal{Q}_t always covers all d_{test} samples, in order to evaluate and compare with other methods equally, which also tests their performance on the entire test subset d_{test} of a dataset d .

HyperFast

The traditional training process can be seen as a function $f(X, Y) = \theta$, that receives training instances $X \in \mathbb{R}^{N \times D}$ and corresponding labels $Y \in \mathbb{R}^N$, and produces a set of trained weights θ of a model. In this work, we substitute the training process with HyperFast, a pre-trained meta-model based on a hypernetwork (Ha, Dai, and Le 2017) h , that takes as input a subset of the training data (i.e. support set \mathcal{S}_t) for a task $t \in \mathcal{T}_{\text{meta-train}}$ and predicts the weights of a main neural network f_θ for the given task t as $\theta^* = h(\mathcal{S}_t)$. The target model $f_{h(\mathcal{S}_t)}$ directly uses the predicted weights and makes predictions for test data points $x \in \mathcal{Q}_t$ in a single forward pass, such that $P_\theta(y|x, \mathcal{S}) = f_{h(\mathcal{S})}(x)$.

The meta-model is learnt by observing a set of tasks $t \in \mathcal{T}_{\text{meta-train}}$ and minimizing $\mathcal{L}_t(f_{h(\mathcal{S})}(x))$. In this section, we detail the design and architecture of h , named HyperFast in analogy to Hypernetworks (Ha, Dai, and Le 2017), and the ability to instantly adapt to new datasets in a single forward pass. Figure 1 illustrates the HyperFast framework and the main building blocks of the architecture. HyperFast is a multi-stage model with initial transformation layers that allows variable input size and permutation invariance, and a combination of linear layers and pooling operations that take both support samples and their associated labels to directly predict the weights θ_{main_l} (weight matrix and bias) of linear layers $l \in [1, L]$ of a target neural network. All trainable modules of HyperFast are learnt end-to-end by optimizing the classification loss of the main network evaluated on \mathcal{Q}_t .

The framework and HyperFast architecture proposed in this paper is a specific instance of a more general framework that could be easily extended to predict convolutional layers, batch normalization layers, recurrent layers, or deeper networks, for example. However, the architecture design depicted in Figure 1 selection has been driven by a global and simple approach to handle a wide range of multi-domain data, while seeking efficiency and speed.

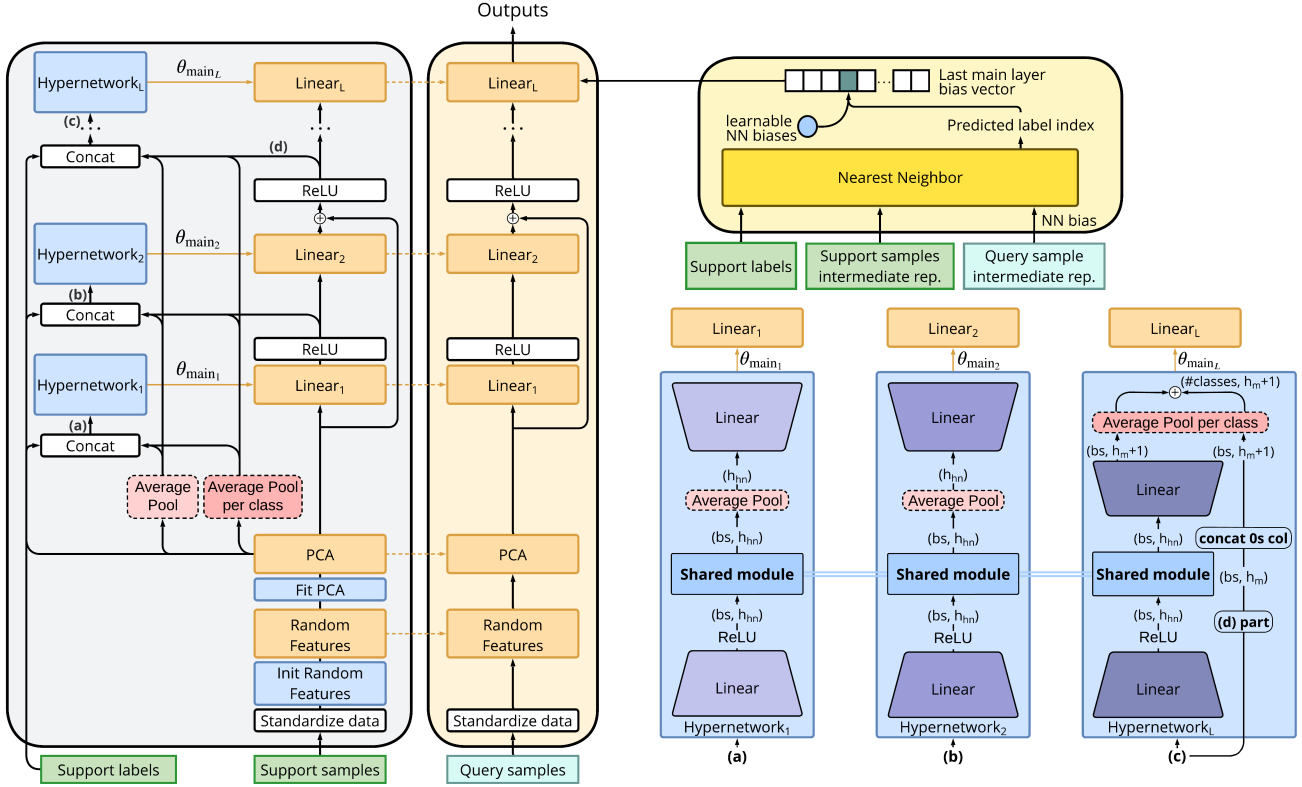


Figure 1: (left) HyperFast framework. (right) Architecture detail. Each hypernetwork module receives representations of the support set of *batch size* (bs) samples. The modules $l \in [1, L - 1]$ compress the representations into a single embedding of *hypernetwork hidden size* (h_{hn}) to then generate the main network weights θ_{main_l} . Module L summarizes the representations per class with embeddings of *main hidden size* (h_m) + 1, directly obtaining the weights of the last classification layer θ_{main_L} .

Initial Transformation Layers

Properly dealing with datasets of differing dimensionality is a challenge, and one common solution is to apply padding (Hollmann et al. 2023) or to keep a subset of selected features up to a fixed size. We first perform a general data standardization stage by one-hot encoding categorical features, mean imputing missing numerical features, mode imputing missing categorical features, and feature-wise transforming to zero mean and unit variance. Then, HyperFast comprises initial layers that project datasets of different dimensionality to fixed-size and feature-permutation invariant representations. The kernel trick can be used to project data to a Reproducing Kernel Hilbert Space (RKHS) (Aronszajn 1950) when the number of dimensions tends to infinity. However, this would require computing all pairwise kernel distance in every step of the training process. Instead, we use random features (RF) (Rahimi and Recht 2007) to approximate a kernel with a fixed and finite number of dimensions. Random features are computed as $\phi(x) = a(Wx)$, where $a(\cdot)$ is a non-linearity, and W is a random projection matrix that follows a pre-defined distribution. The approximated kernel depends on the distribution of W and the selected non-linearity. In our case, we sample W from a Gaussian distribution and use the ReLU activation

as non-linearity, approximating an arc-cosine kernel. We choose to approximate the arc-cosine kernel because it captures sparse, neural network-like feature representations in a non-parametric kernel setting (Cho and Saul 2009). In contrast, polynomial kernel’s features are neither sparse nor non-negative, and radial basis function (RBF) kernels capture localized similarities. In each forward step, the random features projection matrix is re-initialized and sampled. The number of rows is adjusted to match the dimensionality of the input dataset, while the number of columns remains fixed, determining the output size.

The combination of random features with Principal Component Analysis (PCA) provides an efficient low-rank randomized approximation of Kernel PCA (Sriperumbudur and Sterge 2017; Lopez-Paz et al. 2014). We estimate the PCA parameters ψ using the support set and project the data onto a specified number of components. Subsequently, both ϕ and ψ are applied to the query samples to transform the data. This transformed data is then forwarded through the L generated linear layers of the main network.

Hypernetwork Modules

The process of generating the weights of the main network is done layer-by-layer, by multiple hypernetwork modules with both shared and layer-specific parameters, see Figure 1.

The hypernetwork module that generates the weights for the main network layer l receives as input the representations of the support samples in the previous stage, concatenated with the one-hot encoded support labels, the global average, and the class average of the low-rank Kernel PCA projection of the support set. Note that each sample is concatenated with the class average corresponding to its associated label.

For predicting θ_{main_1} , the representations are the low-rank Kernel PCA projection of the support samples. For $\theta_{\text{main}_l} \in [2, L]$, the hypernetwork module receives the intermediate representations of the support set in the main network at the output of layer $l - 1$, after non-linearities and residual connections are applied. Figure 1 represents a specific multi-layer perceptron (MLP) architecture with ReLU activations and residual connections, which we use for our experiments. However, the HyperFast framework can be easily extended to generate weights for other main network architectures.

The hypernetwork modules that predict the layers $l \in [1, L - 1]$ are composed of MLPs with shared middle layers that take the support set representations and labels, and output embeddings for each sample in the support set. Then, permutation-invariant weights are obtained averaging all support embeddings in a similar fashion to Deep Sets (Zaheer et al. 2017), to obtain a single dataset embedding that is passed to a final linear layer which outputs the final weights θ_{main_l} of l . θ_{main_l} is then reshaped as weight matrix and bias vector to forward the data through the main network.

Layer L is the classification layer of the main layer that outputs the logits for the final prediction. In this case, the intermediate representations after the layer $L - 1$ and labels information are encoded through a MLP hypernetwork but the weights θ_{main_L} are not directly predicted from a global embedding. Instead, we leverage the fact that the rows of the classification layer weight matrix correspond to the different categories of the task. We perform an average pooling per class, and obtain the rows of the classification weight matrix (and bias) as the average of representations for each category. This also allows a much lightweight implementation, instead of directly predict the weight matrix. Additionally, we add a residual connection (He et al. 2016) from the previous layer representations for which we also perform a per class average, which helps in retaining category information from the input. Finally, we consider a module based on Nearest Neighbors to add learnable parameters (NN biases) to the classification layer bias vector of the main network. The label of a query sample is predicted with NN using the support set and the intermediate representations of the data across the main network, such that $P_\theta(y|x, \mathcal{S}) = f_{h(\mathcal{S})}(x, \mathcal{S})$. We consider the representations after the PCA projection, and after each linear layer. The NN biases are added to the position of the bias of the last main classification layer corresponding to the predicted label.

Once the main network is fully generated, query samples can be forwarded to make predictions. During meta-training, the predictions for the query samples \mathcal{Q}_t of $t \in \mathcal{T}_{\text{meta-train}}$ are used to compute the cross-entropy loss \mathcal{L}_t and learn the parameters of HyperFast end-to-end. In evaluation, all hypernetwork parameters are frozen and generate weights for a main network in a single forward pass.

Experiments

In this section, we compare HyperFast to many standard ML methods, AutoML systems and DL methods for tabular data on a wide variety of tabular classification tasks, listed in the Appendix. We do not perform any hyperparameter tuning to HyperFast, as it can be used as an off-the-shelf hypernetwork ready to generate networks to perform inference on new datasets. We then compare the performance and runtime of the generated model in a single forward pass, as well as the combination of multiple generated networks by increasing the ensemble size and fine-tuning on inference.

Baselines We compare HyperFast to standard ML methods, AutoML systems and state-of-the-art DL methods for tabular data. We first consider simple and fast ML methods as K -Nearest Neighbors (KNN) and Logistic Regression (Log. Reg.), and a MLP matching the architecture of the target network. We also evaluate against tree-based boosting methods: XGBoost (Chen and Guestrin 2016), LightGBM (Ke et al. 2017), and CatBoost (Prokhorenkova et al. 2018). As AutoML methods we incorporate Auto-Sklearn 2.0 (ASKL 2.0) (Feurer et al. 2020), which uses Bayesian Optimization to efficiently discover a top-performing ML model or a combination of models by ensembling, and AutoGluon (Erickson et al. 2020), which uses a selection of models such as neural networks, KNN, and tree-based models, combining them into a stacked ensemble. Finally, we include popular tabular DL methods: SAINT (Somepalli et al. 2021), TabPFN (Hollmann et al. 2023), NODE (Popov, Morozov, and Babenko 2019), FT-Transformer (Gorishniy et al. 2021), and T2G-Former (Yan et al. 2023). All standard ML models, gradient boosting methods and SAINT are evaluated using 5-fold cross validation for hyperparameter adjustment. Hyperparameter configurations are drawn from search spaces (detailed in the Appendix) until 10000 configurations are explored, a specified time budget is reached, or more than 32 GB of memory are required if GPU training is possible for the model. Then, the model is trained on the full training set with the best configuration between the hyperparameter search result and the default. For the AutoML methods, the time budget is given. Finally, both TabPFN and our HyperFast are pre-trained models with no hyperparameter tuning requirements, but with ensembling capabilities. Thus, we perform ensembling for each method until a given number of members are used (detailed in the Appendix) or until 32 GB of GPU memory are overloaded.

Data We collect a wide variety of datasets from different modalities. We use the 70 tabular datasets from the OpenML-CC18 suite (Bischl et al. 2021) which, to the best of our knowledge, is the *largest* and most used standardized tabular dataset benchmark, composed of standard classification datasets (e.g., Breast Cancer, Bank Marketing). The collection of OpenML datasets is randomly shuffled and divided into meta-training, meta-validation and meta-testing sets, with a 75%-10%-15% split, respectively. We also include tabular genomics datasets sourced from distinct biobanks. Specifically, we utilize genome sequences of dogs (Bartusiak et al. 2022) for dog clade (group of breeds) prediction in meta-training, European (British) humans from

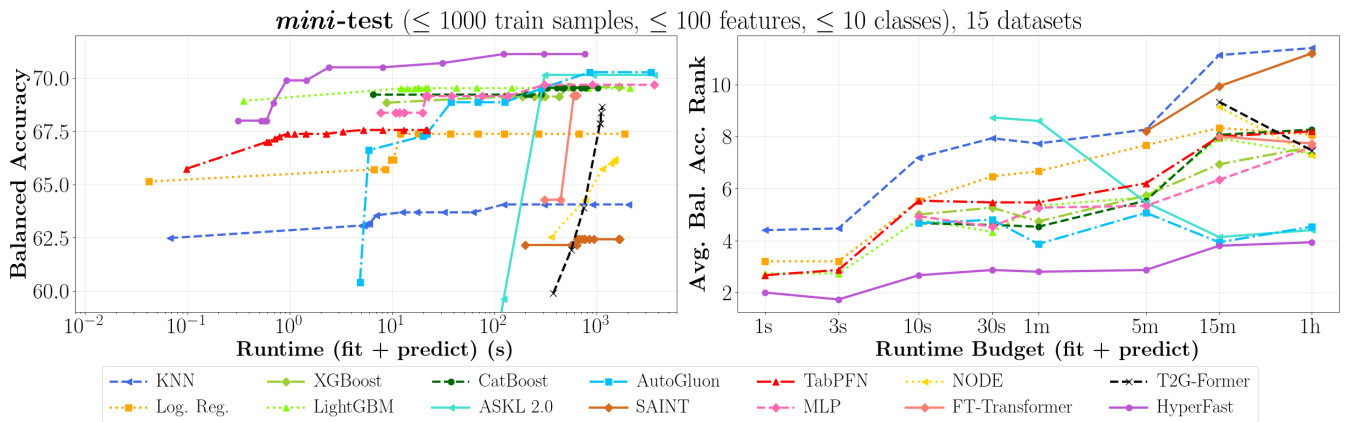


Figure 2: Runtime (fit + predict) vs. performance and average rank for given runtime budgets on the *mini-test* (small-sized version of the 15 meta-test datasets with ≤ 1000 training examples, ≤ 100 features and ≤ 10 classes restrictions).

the UK Biobank (UKB) (Sudlow et al. 2015) for phenotype prediction in meta-validation, and HapMap3 (Consortium et al. 2010) for subpopulation prediction in the meta-test. This strict separation ensures we meta-learn and evaluate on substantially different distributions and tasks. More details on the processing of these datasets are provided in the Appendix. The simple ML methods, implemented with scikit-learn (Pedregosa et al. 2011), and the MLP, receive the numerical features standardized with zero mean and unit variance, and the categorical features are one-hot encoded. For the missing values, we perform mean imputation for numerical features and mode imputation for categorical features, as it was the configuration that yielded the best performance. We also perform imputation of missing values for SAINT, NODE, and FT-Transformer. Boosting methods, AutoML systems, and TabPFN receive the raw data and the indices of categorical features when needed, as their documentation states that they pre-process inputs internally.

Apart from the large-sized original test datasets, we create a secondary small-sized tabular data version (*mini-test*) of the meta-testing datasets to compare to TabPFN, as it is only able to handle ≤ 1000 training examples, ≤ 100 features and ≤ 10 classes. We randomly select a subset of ≤ 1000 training samples and ≤ 100 features for each dataset. We do not perform any downsizing in terms of number of classes as the highest number of classes appearing in the meta-testing set is 10. However, HyperFast is pre-trained with datasets with higher number of classes and can be used in inference for datasets with >10 classes. Only models that can complete the runs for all 15 datasets in less than 48 hours in their default configuration are included in our large-scale experiments. The experiments, which are conducted for all models and both size versions of the 15 meta-testing datasets, considering all time budgets shown in Figure 2, require a total of 2 months to complete. Therefore, we show additional results with 10 repetitions of the experiments for a specific time budget of 5 minutes for each dataset in the Appendix.

Experimental setup We perform supervised classification with HyperFast and all other baselines on the *mini-test*, a

small-sized version of the meta-test datasets $\mathcal{D}_{\text{meta-test}}$, and in the original large-scale datasets. To train HyperFast, we use a different set of meta-training datasets, $\mathcal{D}_{\text{meta-train}}$, and select the model with the best average performance on the meta-validation datasets, $\mathcal{D}_{\text{meta-val}}$. We report balanced accuracy, which is the mean of sensitivity and specificity. Balanced accuracy provides a more objective and robust evaluation across classes, especially in the context of imbalanced datasets. In contrast, standard accuracy can be misleading, often masking poor performance in minority classes. We evaluate the models on a time budget (including tuning, training, and prediction) to correctly assess computational complexity and performance. The average rank is also reported.

In order to transform the data to a fixed-size and permutation invariant representation, we apply Random Features and Principal Component Analysis to both support samples and query samples. We set a Random Features projection to 32768 (2^{15}) features, sampled from a normal distribution following the He initialization (He et al. 2015), followed by a ReLU activation. Note that the random linear layer that computes the random features is not trained, and re-initialized in each HyperFast forward step. Then, we keep the principal components (PCs) associated to the 784 largest eigenvalues, as many of the datasets considered have this dimensionality, and it is a more than sufficient number of dimensions to retain the important information of higher dimensional datasets while preserving efficiency. After the PCA projection, most genomics datasets resemble a similar histogram distribution (i.e., zero mean, small deviation and no outliers). However, it is not the case for some OpenML datasets, which are also centered around zero but present many outliers. Thus, we clip the data after PCA at 4σ .

The hypernetwork modules receive a concatenation of intermediate representations of the support samples, and the support labels. Given that each dataset features a different number of categories and linear layers require a fixed input size, we one-hot encode the labels and apply zero padding up to the maximum number of categories considered in the

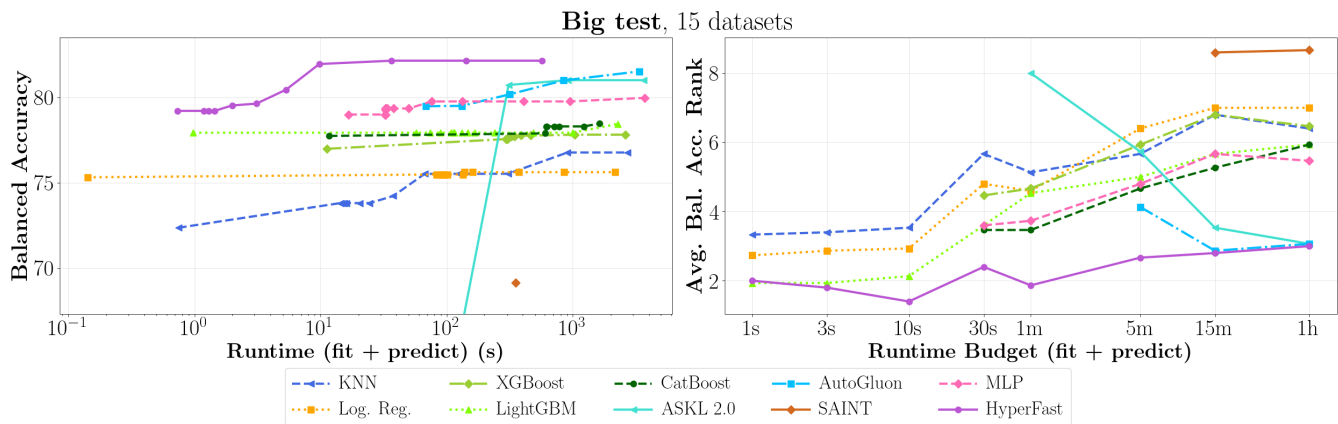


Figure 3: Runtime (fit + predict) vs. performance and average rank for given runtime budgets on the big test: 15 large/medium-sized meta-datasets.

experiments. It is important to note that the number of categories that HyperFast can handle is easily extendable by expanding the input size of HyperFast and zero padding the remaining input dimensions. Such modifications have a negligible impact on efficiency or memory requirements, up to a reasonable number of categories. As a shared module we use 2 feed-forward layers with a hidden size of 1024 and ReLU activations. For the main network, we consider a 3-layer MLP with a residual connection (He et al. 2016), and a main network hidden size equal to the number of PCs (784 dimensions). We select this simple architecture to be able to obtain competitive performance on a wide variety of datasets with a single trained model while preserving efficiency. Other alternatives include predicting weights for CNN layers for only-image datasets, or recurrent layers, for sequential data. Instead, we create a general and simple meta-learning framework to perform fast lightweight inference. In the NN bias module, we randomly select a subset of a maximum of 2048 support samples, since computing all pairwise distances for a large number of datapoints causes high inefficiency and GPU memory overload. A maximum batch size of 2048 samples is used for training, and we make sure to have a sufficient number of samples per category in every case.

In evaluation, we show prediction results with HyperFast in a single forward pass, as well as predictions by ensembling main networks generated in multiple forward passes. We also experiment with performing gradient steps with the training data of the meta-testing datasets on the generated main networks, including the random features projection matrix, PCA parameters and linear layers.

Results on small-sized datasets. We first compare HyperFast to the other methods on a small-sized setting with datasets having ≤ 1000 training samples, ≤ 100 features and ≤ 10 classes, in order to compare to TabPFN. As shown in Figure 2, HyperFast delivers superior results in both performance and runtime, with better prediction capabilities up to 3 orders of magnitude faster than competing methods. Simple ML methods such as KNN and Log. Reg. also deliver

instant predictions, but do not achieve remarkable performance. Interestingly, an MLP (with an architecture identical to the network generated by HyperFast, including the including the initial transformation layers) performs on par with XGBoost. However, HyperFast surpasses gradient-boosting techniques in both runtime and performance. LightGBM stands out as the only boosting machine that achieves a higher balanced accuracy in a similar runtime to a single forward pass by HyperFast. Yet, an ensemble of networks generated by HyperFast outperforms all fine-tuned boosting machines in under 3 seconds. TabPFN is noted for its rapid predictions and outperforms NODE and SAINT. But on average, it falls behind gradient boosting machines and neural models, including HyperFast. FT-Transformer, T2G-Former, NODE, and SAINT are DL tabular models with very time-consuming training, and FT-Transformer obtains the highest performance among them, similar to that of gradient-boosting machines. AutoML systems are superior to the other baselines when given higher runtime budgets. However, HyperFast still outperforms both AutoGluon and ASKL 2.0 for runtimes up to 1h, obtaining the lowest rank throughout all the budgets in the mini test.

Results on medium/large-scale datasets. Figure 3 benchmarks the algorithms on large real-world datasets. We observe that HyperFast is able to obtain predictions in less than a second, and achieves the overall best performance in a wide range of runtime budgets, ranging from 1 second to 5 minutes. For more extended budgets, up to 1h per dataset, HyperFast’s performance is on par with other AutoML systems. Specifically, HyperFast, ASKL 2.0, and AutoGluon all achieve an average rank of approximately 3.0. In comparison, gradient-boosting machines plateau at a balanced accuracy of 78.4% and rank above 5.9, being outperformed by the MLP. SAINT obtains the lowest performance, using the hyperparameter configuration that the authors implement for the biggest datasets they consider in their benchmark. No hyperparameter optimization is performed for SAINT in the big test since larger architectures do not fit in GPU memory for the larger datasets. Additional

Variation	Bal. acc. (%)	Bal. acc. diff.	Fit time (s)	Pred. time (s)	HF size	Model size
Base model (784 PCs)	81.496	-	0.600	0.125	1.27 B	52.65 M
No RF	75.387	-6.108	0.126	0.114	1.27 B	1.85 M
No RF-PCA	73.704	-7.792	0.029	0.109	1.26 B	1.23 M
First 512 PCs only	81.347	-0.149	0.625	0.125	547 M	43.03 M
First 256 PCs only	81.235	-0.261	0.640	0.042	140 M	34.25 M
$d_{RF}=16\,384\ (2^{14})$	81.059	-0.436	0.510	0.116	1.27 B	26.95 M
No concat PCA to hypern. modules	80.727	-0.769	0.583	0.125	1.26 B	52.65 M
1 linear layer in shared module	80.790	-0.706	0.637	0.125	1.27 B	52.65 M
No residual conn. in hypern. L	77.835	-3.660	0.620	0.125	1.27 B	52.65 M
No residual con. in main model	80.318	-1.178	0.633	0.125	1.27 B	52.65 M
No NN bias using PCA features	81.305	-0.191	0.625	0.125	1.27 B	52.65 M
No NN bias using interm. act.	80.703	-0.793	0.628	0.125	1.27 B	52.65 M
No NN biases	79.714	-1.781	0.628	0.125	1.27 B	52.65 M
Random init. linear layers main	72.229	-9.267	0.437	0.125	-	52.65 M

Table 1: Ablation studies on HyperFast performing a single forward pass. Time results are shown for a single GPU. *HF size* denotes the number of trainable parameters of HyperFast, i.e., the meta-model, while *Model size* denotes the size of the generated model.

experiments with very high-dimensional genomic datasets can be found in the appendix.

Ablation Experiments In Table 1, we present ablation studies for the HyperFast framework, exploring variations affecting both hypernetwork modules and the generated model. First, we consider removing the RF and both RF and PCA modules, obtaining a fixed-sized input by keeping the first 784 features or applying zero padding. The weight generation time is reduced from 0.6s to 0.12s and 0.03s, since the main time bottleneck is the RF matrix multiplication and SVD to obtain the PCs. Also, the main model size is greatly reduced as RFs account for most parameters, but the drop in performance is one of the most significant. This is because RF and PCA not only allow transforming any dataset to a fixed number of features, but also homogenize the input data to HyperFast and the generated network across datasets. For example, the first feature post RF-PCA holds the most variance, with subsequent features capturing the maximum variance that is orthogonal to the previous dimensions, with minimal information loss. Also, histogram distributions are similar across datasets with zero mean. These properties help in learning important meta-features across different dataset distributions. If we scale down RF-PCA by reducing the number of PCs used and the RF dimensionality, we observe that model size is significantly reduced while the drop in performance is not critical, which shows that most dataset relevant information is preserved, even using 512 or 256 PCs. These observations can help create even more efficient HyperFast designs in the future. In addition, PCA representations concatenated to hypernetwork inputs retain key information without a major parameter increase. We also observe that reducing the shared hypernetwork module from 2 to 1 layer degrades performance, and residual connections in both the hypernetwork and main model are key to retain post-PCA and per class information, while not increasing model size and runtime. We also analyze the retrieval-based

component of HyperFast. We observe that NN biases in the last classification layer improve predictions while maintaining model size, especially using the intermediate activations of the main network as features. Finally, if we replace the weights produced by HyperFast by random weights, and base the prediction solely on the Nearest Neighbor-based component, we observe the biggest drop in performance.

Conclusion

We present HyperFast, a meta-trained hypernetwork designed to perform rapid classification of tabular data by encoding task information in the prediction of the weights of a target network in a single forward pass. Our experiments show that HyperFast consistently improves performance over traditional ML methods and tabular-specific DL architectures in a matter of seconds. Remarkably, it is able to replace the traditional training of a neural network, and achieves competitive results with state-of-the-art AutoML frameworks trained for 1h. HyperFast eliminates the necessity for time-consuming hyperparameter tuning, making it a highly accessible, off-the-shelf model that can be specially useful for fast classification tasks. We also explore how we can leverage all training data by creating ensembles of generated networks and fine-tuning them on inference, significantly boosting performance at almost no additional computational cost. Future work should consider expanding this framework to a general architecture or multi-hypernetwork setting that is able to handle regression tasks, multi-domain and high-dimensional non-tabular settings such as audio streams, 3D, and video.

Acknowledgments

This work was partially supported by a grant from the Stanford Institute for Human-Centered Artificial Intelligence (HAI) and by NIH under award R01HG010140. This research has been conducted using the UK Biobank Resource under Application Number 24983.

References

- Arik, S. O.; and Pfister, T. 2021. TabNet: Attentive Interpretable Tabular Learning. *Proceedings of the AAAI Conference on Artificial Intelligence*, 35(8): 6679–6687.
- Aronszajn, N. 1950. Theory of reproducing kernels. *Transactions of the American mathematical society*, 68(3): 337–404.
- Ashkenazi, M.; Rimon, Z.; Vainshtein, R.; Levi, S.; Richardson, E.; Mintz, P.; and Treister, E. 2022. NeRN – Learning Neural Representations for Neural Networks.
- Bartusiak, E. R.; Barrabés, M.; Rymbekova, A.; Gimbernat-Mayol, J.; López, C.; Barberis, L.; Montserrat, D. M.; Giró-I-Nieto, X.; and Ioannidis, A. G. 2022. Predicting Dog Phenotypes from Genotypes. In *2022 44th Annual International Conference of the IEEE Engineering in Medicine & Biology Society (EMBC)*, 3558–3562.
- Bergstra, J.; Komer, B.; Eliasmith, C.; Yamins, D.; and Cox, D. D. 2015. Hyperopt: a python library for model selection and hyperparameter optimization. *Computational Science & Discovery*, 8(1): 014008.
- Bischi, B.; Casalicchio, G.; Feurer, M.; Gijbbers, P.; Hutter, F.; Lang, M.; Mantovani, R. G.; van Rijn, J. N.; and Vanschoren, J. 2021. OpenML Benchmarking Suites. In *Thirty-fifth Conference on Neural Information Processing Systems Datasets and Benchmarks Track (Round 2)*.
- Bonet, D.; Levin, M.; Montserrat, D. M.; and Ioannidis, A. G. 2024. Machine Learning Strategies for Improved Phenotype Prediction in Underrepresented Populations. In *Pacific Symposium on Biocomputing. Pacific Symposium on Biocomputing*, volume 29, 404–418.
- Borisov, V.; Leemann, T.; Seßler, K.; Haug, J.; Pawelczyk, M.; and Kasneci, G. 2021. Deep Neural Networks and Tabular Data: A Survey. *CoRR*, abs/2110.01889.
- Chen, J.; Liao, K.; Fang, Y.; Chen, D.; and Wu, J. 2022a. TabCaps: A Capsule Neural Network for Tabular Data Classification with BoW Routing. In *International Conference on Learning Representations*.
- Chen, J.; Liao, K.; Wan, Y.; Chen, D. Z.; and Wu, J. 2022b. Danets: Deep abstract networks for tabular data classification and regression. *Proceedings of the AAAI Conference on Artificial Intelligence*, 36(4): 3930–3938.
- Chen, J.; Yan, J.; Chen, D. Z.; and Wu, J. 2023. ExcelFormer: A Neural Network Surpassing GBDTs on Tabular Data. *arXiv preprint arXiv:2301.02819*.
- Chen, T.; and Guestrin, C. 2016. XGBoost: A Scalable Tree Boosting System. In *Proceedings of the 22nd ACM SIGKDD International Conference on Knowledge Discovery and Data Mining, KDD '16*, 785–794. New York, NY, USA: Association for Computing Machinery. ISBN 9781450342322.
- Cho, Y.; and Saul, L. 2009. Kernel Methods for Deep Learning. In Bengio, Y.; Schuurmans, D.; Lafferty, J.; Williams, C.; and Culotta, A., eds., *Advances in Neural Information Processing Systems*, volume 22. Curran Associates, Inc.
- Consortium, I. H. .; et al. 2010. Integrating common and rare genetic variation in diverse human populations. *Nature*, 467(7311): 52.
- Deiana, A. M.; Tran, N.; Agar, J.; Blott, M.; Di Guglielmo, G.; Duarte, J.; Harris, P.; Hauck, S.; Liu, M.; Neubauer, M. S.; et al. 2022. Applications and techniques for fast machine learning in science. *Frontiers in big Data*, 5: 787421.
- Deutsch, L. 2018. Generating neural networks with neural networks. *arXiv preprint arXiv:1801.01952*.
- Duda, R. O.; Hart, P. E.; and Stork, D. G. 2000. *Pattern Classification (2nd Edition)*. USA: Wiley-Interscience. ISBN 0471056693.
- Erickson, N.; Mueller, J.; Shirkov, A.; Zhang, H.; Larroy, P.; Li, M.; and Smola, A. 2020. Autoglouon-tabular: Robust and accurate autotml for structured data. *arXiv preprint arXiv:2003.06505*.
- Esteva, A.; Robicquet, A.; Ramsundar, B.; Kuleshov, V.; DePristo, M.; Chou, K.; Cui, C.; Corrado, G.; Thrun, S.; and Dean, J. 2019. A guide to deep learning in healthcare. *Nature medicine*, 25(1): 24–29.
- Feurer, M.; Eggenberger, K.; Falkner, S.; Lindauer, M.; and Hutter, F. 2020. Auto-Sklearn 2.0: Hands-free AutoML via Meta-Learning. *arXiv:2007.04074 [cs.LG]*.
- Finn, C.; Abbeel, P.; and Levine, S. 2017. Model-agnostic meta-learning for fast adaptation of deep networks. In *International conference on machine learning*, 1126–1135. PMLR.
- Garnelo, M.; Rosenbaum, D.; Maddison, C.; Ramalho, T.; Saxton, D.; Shanahan, M.; Teh, Y. W.; Rezende, D.; and Eslami, S. A. 2018a. Conditional neural processes. In *International Conference on Machine Learning*, 1704–1713. PMLR.
- Garnelo, M.; Schwarz, J.; Rosenbaum, D.; Viola, F.; Rezende, D. J.; Eslami, S.; and Teh, Y. W. 2018b. Neural processes. *ICML Workshop on Theoretical Foundations and Applications of Deep Generative Models*.
- Gidaris, S.; and Komodakis, N. 2018. Dynamic few-shot visual learning without forgetting. In *Proceedings of the IEEE conference on computer vision and pattern recognition*, 4367–4375.
- Gorishniy, Y.; Rubachev, I.; Khurlov, V.; and Babenko, A. 2021. Revisiting deep learning models for tabular data. *Advances in Neural Information Processing Systems*, 34: 18932–18943.
- Grinsztajn, L.; Oyallon, E.; and Varoquaux, G. 2022. Why do tree-based models still outperform deep learning on typical tabular data? In *Thirty-sixth Conference on Neural Information Processing Systems Datasets and Benchmarks Track*.
- Ha, D.; Dai, A. M.; and Le, Q. V. 2017. HyperNetworks. In *ICLR*.
- He, K.; Zhang, X.; Ren, S.; and Sun, J. 2015. Delving deep into rectifiers: Surpassing human-level performance on imagenet classification. In *Proceedings of the IEEE international conference on computer vision*, 1026–1034.
- He, K.; Zhang, X.; Ren, S.; and Sun, J. 2016. Deep residual learning for image recognition. In *Proceedings of the IEEE conference on computer vision and pattern recognition*, 770–778.

- He, X.; Zhao, K.; and Chu, X. 2021. AutoML: A survey of the state-of-the-art. *Knowledge-Based Systems*, 212: 106622.
- Hollmann, N.; Müller, S.; Eggensperger, K.; and Hutter, F. 2023. TabPFN: A Transformer That Solves Small Tabular Classification Problems in a Second. In *The Eleventh International Conference on Learning Representations*.
- Kadra, A.; Lindauer, M.; Hutter, F.; and Grabocka, J. 2021. Well-tuned Simple Nets Excel on Tabular Datasets. In Ranzato, M.; Beygelzimer, A.; Dauphin, Y.; Liang, P.; and Vaughan, J. W., eds., *Advances in Neural Information Processing Systems*, volume 34, 23928–23941. Curran Associates, Inc.
- Katzir, L.; Elidan, G.; and El-Yaniv, R. 2020. Net-dnf: Effective deep modeling of tabular data. In *International Conference on Learning Representations*.
- Ke, G.; Meng, Q.; Finley, T.; Wang, T.; Chen, W.; Ma, W.; Ye, Q.; and Liu, T.-Y. 2017. LightGBM: A Highly Efficient Gradient Boosting Decision Tree. In Guyon, I.; Luxburg, U. V.; Bengio, S.; Wallach, H.; Fergus, R.; Vishwanathan, S.; and Garnett, R., eds., *Advances in Neural Information Processing Systems*, volume 30. Curran Associates, Inc.
- Komer, B.; Bergstra, J.; and Eliasmith, C. 2014. Hyperopt-sklearn: automatic hyperparameter configuration for scikit-learn. In *ICML workshop on AutoML*, volume 9, 50. Citeseer Austin, TX.
- Kossen, J.; Band, N.; Lyle, C.; Gomez, A. N.; Rainforth, T.; and Gal, Y. 2021. Self-attention between datapoints: Going beyond individual input-output pairs in deep learning. *Advances in Neural Information Processing Systems*, 34: 28742–28756.
- Krueger, D.; Huang, C.-W.; Islam, R.; Turner, R.; Lacoste, A.; and Courville, A. 2018. Bayesian Hypernetworks.
- Lopez-Paz, D.; Sra, S.; Smola, A.; Ghahramani, Z.; and Schölkopf, B. 2014. Randomized nonlinear component analysis. In *International conference on machine learning*, 1359–1367. PMLR.
- Loshchilov, I.; and Hutter, F. 2018. Decoupled Weight Decay Regularization. In *International Conference on Learning Representations*.
- Louizos, C.; and Welling, M. 2017. Multiplicative Normalizing Flows for Variational Bayesian Neural Networks. In *Proceedings of the 34th International Conference on Machine Learning - Volume 70, ICML'17*, 2218–2227. JMLR.org.
- McElfresh, D.; Khandagale, S.; Valverde, J.; Ramakrishnan, G.; Goldblum, M.; White, C.; et al. 2023. When Do Neural Nets Outperform Boosted Trees on Tabular Data? *arXiv preprint arXiv:2305.02997*.
- Mildenhall, B.; Srinivasan, P. P.; Tancik, M.; Barron, J. T.; Ramamoorthi, R.; and Ng, R. 2020. NeRF: Representing Scenes as Neural Radiance Fields for View Synthesis. In *ECCV*.
- Novembre, J.; Johnson, T.; Bryc, K.; Kutalik, Z.; Boyko, A. R.; Auton, A.; Indap, A.; King, K. S.; Bergmann, S.; Nelson, M. R.; et al. 2008. Genes mirror geography within Europe. *Nature*, 456(7218): 98–101.
- Pedregosa, F.; Varoquaux, G.; Gramfort, A.; Michel, V.; Thirion, B.; Grisel, O.; Blondel, M.; Prettenhofer, P.; Weiss, R.; Dubourg, V.; Vanderplas, J.; Passos, A.; Cournapeau, D.; Brucher, M.; Perrot, M.; and Duchesnay, E. 2011. Scikit-learn: Machine Learning in Python. *Journal of Machine Learning Research*, 12: 2825–2830.
- Popov, S.; Morozov, S.; and Babenko, A. 2019. Neural oblivious decision ensembles for deep learning on tabular data. *arXiv preprint arXiv:1909.06312*.
- Prokhorenkova, L.; Gusev, G.; Vorobev, A.; Dorogush, A. V.; and Gulin, A. 2018. CatBoost: unbiased boosting with categorical features. In Bengio, S.; Wallach, H.; Larochelle, H.; Grauman, K.; Cesa-Bianchi, N.; and Garnett, R., eds., *Advances in Neural Information Processing Systems*, volume 31. Curran Associates, Inc.
- Qian, J.; Tanigawa, Y.; Du, W.; Aguirre, M.; Chang, C.; Tibshirani, R.; Rivas, M. A.; and Hastie, T. 2020. A fast and scalable framework for large-scale and ultrahigh-dimensional sparse regression with application to the UK Biobank. *PLoS genetics*, 16(10): e1009141.
- Qiao, S.; Liu, C.; Shen, W.; and Yuille, A. L. 2018. Few-shot image recognition by predicting parameters from activations. In *Proceedings of the IEEE conference on computer vision and pattern recognition*, 7229–7238.
- Rahimi, A.; and Recht, B. 2007. Random features for large-scale kernel machines. *Advances in neural information processing systems*, 20.
- Ratzlaff, N.; and Fuxin, L. 2019. HyperGAN: A Generative Model for Diverse, Performant Neural Networks. In Chaudhuri, K.; and Salakhutdinov, R., eds., *Proceedings of the 36th International Conference on Machine Learning*, volume 97 of *Proceedings of Machine Learning Research*, 5361–5369. PMLR.
- Schürholt, K.; Knyazev, B.; i Nieto, X. G.; and Borth, D. 2022. Hyper-Representations as Generative Models: Sampling Unseen Neural Network Weights. In Oh, A. H.; Agarwal, A.; Belgrave, D.; and Cho, K., eds., *Advances in Neural Information Processing Systems*.
- Shwartz-Ziv, R.; and Armon, A. 2022. Tabular Data: Deep Learning is Not All You Need. *Inf. Fusion*, 81(C): 84–90.
- Snell, J.; Swersky, K.; and Zemel, R. 2017. Prototypical networks for few-shot learning. *Advances in neural information processing systems*, 30.
- Somepalli, G.; Goldblum, M.; Schwarzschild, A.; Bruss, C. B.; and Goldstein, T. 2021. SAINT: Improved neural networks for tabular data via row attention and contrastive pre-training. *arXiv preprint arXiv:2106.01342*.
- Sriperumbudur, B.; and Sterge, N. 2017. Approximate kernel PCA using random features: Computational vs. statistical trade-off. *arXiv preprint arXiv:1706.06296*.
- Stanley, K. O.; D’Ambrosio, D. B.; and Gauci, J. 2009. A hypercube-based encoding for evolving large-scale neural networks. *Artificial life*, 15(2): 185–212.
- Sudlow, C.; Gallacher, J.; Allen, N.; Beral, V.; Burton, P.; Danesh, J.; Downey, P.; Elliott, P.; Green, J.; Landray, M.;

et al. 2015. UK biobank: an open access resource for identifying the causes of a wide range of complex diseases of middle and old age. *PLoS medicine*, 12(3): e1001779.

Tanigawa, Y.; Qian, J.; Venkataraman, G.; Justesen, J. M.; Li, R.; Tibshirani, R.; Hastie, T.; and Rivas, M. A. 2022. Significant sparse polygenic risk scores across 813 traits in UK Biobank. *PLoS Genetics*, 18(3): e1010105.

Vinyals, O.; Blundell, C.; Lillicrap, T.; Wierstra, D.; et al. 2016. Matching networks for one shot learning. *Advances in neural information processing systems*, 29.

Yan, J.; Chen, J.; Wu, Y.; Chen, D. Z.; and Wu, J. 2023. T2g-former: organizing tabular features into relation graphs promotes heterogeneous feature interaction. *Proceedings of the AAAI Conference on Artificial Intelligence*, 37(9): 10720–10728.

Yang, Q.; Liu, Y.; Cheng, Y.; Kang, Y.; Chen, T.; and Yu, H. 2019. Federated learning. *Synthesis Lectures on Artificial Intelligence and Machine Learning*, 13(3): 1–207.

Zaheer, M.; Kottur, S.; Ravanbakhsh, S.; Poczos, B.; Salakhutdinov, R. R.; and Smola, A. J. 2017. Deep sets. *Advances in neural information processing systems*, 30.

Zhang, T.; Wang, S.; Yan, S.; Li, J.; and Liu, Q. 2023. Generative Table Pre-training Empowers Models for Tabular Prediction. *arXiv preprint arXiv:2305.09696*.

Zhmoginov, A.; Sandler, M.; and Vladymyrov, M. 2022. Hypertransformer: Model generation for supervised and semi-supervised few-shot learning. In *ICML*, 27075–27098.

Zhu, B.; Shi, X.; Erickson, N.; Li, M.; Karypis, G.; and Shoaran, M. 2023. XTab: Cross-table Pretraining for Tabular Transformers. *arXiv preprint arXiv:2305.06090*.

Experimental Setup

Datasets

OpenML We integrate the OpenML Curated Classification benchmarking suite 2018 (OpenML-CC18) (Bischl et al. 2021). OpenML-CC18 consists of 72 diverse and curated classification tasks, and we keep 70 datasets, excluding the vision datasets Fashion-MNIST and CIFAR-10. We split each dataset into 80% train and 20% test.

HapMap3 HapMap3 (Consortium et al. 2010) is a publicly available dataset that contains single-nucleotide polymorphisms (SNPs) sequences of whole-genome data from humans with subpopulation annotations. Samples are filtered for the 10 largest human subpopulations, which are used as categories for the *hapmap* datasets. Individuals are split into 75% for train and 25% for test. SNPs with missing values for any sample are discarded. Finally, 5 different datasets are created by randomly sampling 784 SNP positions from different sections of the chromosomes, which are encoded as binary values. For every created dataset, labels are permuted to avoid overfitting to the positions of the labels of each subpopulation.

Dogs Similarly, Dogs (Bartusiak et al. 2022) is a dataset of dog DNA sequences. The dataset consists of the genotyping array of purebred dogs from 75 breeds. Dog breeds can be organized into clades, which are groups of dog breeds that share a common ancestor. Since the number of samples per breed in the dataset is very low, breeds are clustered into clades, and the 10 most common clades are kept and used as categories for the *dogs* datasets. Samples are split into 75% for train and 25% for test. SNPs with missing values for any sample are discarded. Finally, 30 different datasets are created by randomly sampling 784 positions from different sections of the chromosomes. For every created dataset, labels are permuted to avoid overfitting to the positions of the labels of each clade.

UK Biobank The UK Biobank (Sudlow et al. 2015) is a large-scale biobank, from which we use the genotyping array data and full phenotypes as processed in (Qian et al. 2020). We include 8 of the most predictive binary phenotypes according to their polygenic risk score (PRS) model:

- Hair colour (natural, before greying) red: *red hair*
- Hair colour (natural, before greying) blonde: *blonde hair*
- Hair colour (natural, before greying) dark brown: *dark brown hair*
- Hair colour (natural, before greying) black: *black hair*
- Ease of skin tanning (Never tan, only burn): *skin burn*
- Ease of skin tanning (Get very tanned): *skin tan*
- Hair colour (natural, before greying) brown: *brown hair*
- Malabsorption/coeliac disease: *malabsorption-coeliac*

In order to allow proper phenotype prediction modeling, it is a standard practice to stick to a single population, to avoid the prediction being biased by other factors. In this case, we filter by the majority population in the UK Biobank, which is British individuals with European ancestry. Then, we create a balanced dataset for each phenotype by selecting all

samples of the minority class (presence of the phenotype), and randomly selecting the same number of samples from the majority class. Variants (features) are selected based on the PRS model weights reported (Tanigawa et al. 2022). We split each dataset into 80% train and 20% test.

The collection of OpenML datasets is randomly shuffled and divided into meta-training (Table 2), meta-validation (Table 3), and meta-testing (Table 4) sets, with a 75%-10%-15% split, respectively. Dogs datasets for dog clade (group of breeds) prediction are used in meta-training, British humans datasets from the UK Biobank (UKB) for phenotype prediction are used in meta-validation, and HapMap3 datasets for subpopulation prediction are used in the meta-test. This strict separation ensures we meta-learn and evaluate on substantially different distributions and tasks.

HyperFast and Baselines Implementation

HyperFast Training Details In the meta-training stage, HyperFast weights are learnt by generating the weights of a smaller model that solves a different training task $t \in \mathcal{T}_{\text{meta-train}}$ at each training step. t is derived from a randomly selected dataset d from the collection of meta-training datasets $\mathcal{D}_{\text{meta-train}}$. However, the gradient signal is too noisy for weight updates at every training step. We fix this issue by accumulating gradients across different tasks before performing an optimization step. We experiment with gradient accumulation of 2, 3, 5, 10, 25, 50, and 100 steps. In our experiments we find that, in general, a larger number of accumulation steps always yields a more stable loss curve. That is, the meta-model learns better from observing the variations across different datasets, rather than solving one task at a time. We use a total of 25 gradient accumulation steps, which already allows a stable training, without excessively prolonging convergence. Despite this, during meta-validation, we observe a tendency to overfit to the meta-training datasets over very long training times. We select the HyperFast model that achieves the best average performance across the meta-validation datasets. We also experimented with solving multiple tasks in a single pass, but it was not possible in many cases due to memory constraints. Another key architectural design choice that significantly stabilizes the training process is sharing the core parameters between hypernetwork modules. As a shared module we use 2 feed-forward layers with a hidden dimensionality of 1024 and ReLU activations. We also experimented with deeper shared modules and different architectures based on attention mechanisms and convolutions, however, training stability and model generalization were inferior. The HyperFast used in this work has 1.27 B parameters (4.7 GB of memory), which generates the weights of smaller models of 52.65 M parameters (200.8 MB). The model is trained for 100,000 steps with a learning rate of 0.0003 with the AdamW optimizer (Loshchilov and Hutter 2018), which required 20 hours on a single NVIDIA Tesla V100 SXM2 GPU.

HyperFast Inference Details Once HyperFast is trained, the hypernetwork weights are frozen and HyperFast can be used as an off-the-shelf model to generate target networks. Significant improvements in performance can be achieved

Dataset name	Train size	Test size	Feature size	Categorical	Classes
dogs _{1..30} (30)	1372	458	784	784	10
sick	3017	755	29	22	2
Bioresponse	3000	751	1776	0	2
splice	2552	638	60	60	3
qsar-biodeg	844	211	41	0	2
MiceProtein	864	216	77	0	8
isolet	6237	1560	617	0	26
connect-4	54045	13512	42	42	3
analcatauthorship	672	169	70	0	4
kr-vs-kp	2556	640	36	36	2
optdigits	4496	1124	64	0	10
analcata_dmft	637	160	4	4	6
churn	4000	1000	20	4	2
mfeat-karhunen	1600	400	64	0	10
mfeat-factors	1600	400	216	0	10
kc1	1687	422	21	0	2
texture	4400	1100	40	0	11
Internet-Advertisements	2623	656	1558	1555	2
har	8239	2060	561	0	6
jungle_chess_2pcs_raw_endgame_complete	35855	8964	6	0	3
car	1382	346	6	6	4
credit-g	800	200	20	13	2
adult	39073	9769	14	8	2
nomao	27572	6893	118	29	2
jm1	8708	2177	21	0	2
numera128.6	77056	19264	21	0	2
first-order-theorem-proving	4894	1224	51	0	6
dna	2548	638	180	180	3
Devnagari-Script	73600	18400	1024	0	46
mfeat-morphological	1600	400	6	0	10
madelon	2080	520	500	0	2
pc3	1250	313	37	0	2
blood-transfusion-service-center	598	150	4	0	2
vehicle	676	170	18	0	4
vowel	792	198	12	2	11
balance-scale	500	125	4	0	3
segment	1848	462	16	0	7
pc1	887	222	21	0	2
tic-tac-toe	766	192	9	9	2
semeion	1274	319	256	0	10
letter	16000	4000	16	0	26
electricity	36249	9063	8	1	2
GesturePhaseSegmentationProcessed	7898	1975	32	0	5
cnae-9	864	216	856	0	9
ozone-level-8hr	2027	507	72	0	2
ilpd	466	117	10	1	2
wall-robot-navigation	4364	1092	24	0	4
mfeat-fourier	1600	400	76	0	10
spambase	3680	921	57	0	2
mnist_784	56000	14000	784	0	10
PhishingWebsites	8844	2211	30	30	2
climate-model-simulation-crashes	432	108	18	0	2
steel-plates-fault	1552	389	27	0	7
mfeat-pixel	1600	400	240	0	10

Table 2: Meta-training datasets $\mathcal{D}_{\text{meta-train}}$. Train size is the number of training instances in d_{train} , and Test size is the number of test instances in d_{test} . Subscripts $i..j$ and (\cdot) denote the interval of indices and the total number of datasets of the same group used, respectively.

Dataset name	Train size	Test size	Feature size	Categorical	Classes
cylinder-bands	432	108	37	19	2
wdbc	455	114	30	0	2
eucalyptus	588	148	19	5	5
mfeat-zernike	1600	400	47	0	10
cmc	1178	295	9	7	3
dresses-sales	400	100	12	11	2
breast-w	559	140	9	0	2
red hair	24638	6160	1621	1621	2
blonde hair	62297	15575	6968	6968	2
dark brown hair	202459	50615	5662	5662	2
black hair	23001	5751	1649	1649	2
skin burn	94972	23744	3158	3158	2
skin tan	108592	27148	4130	4130	2
brown hair	114502	28626	4024	4024	2
malabsorption-coeliac	3672	918	423	423	2

Table 3: Meta-validation datasets $\mathcal{D}_{\text{meta-val}}$. Train size is the number of training instances in d_{train} , and Test size is the number of test instances in d_{test} .

Dataset name	Train size	Test size	Feature size	Categorical	Classes
hapmap1..5 (5)	1660	554	784	784	10
phoneme	4323	1081	5	0	2
wilt	3871	968	5	0	2
pendigits	8793	2199	16	0	10
satimage	5144	1286	36	0	6
credit-approval	552	138	15	9	2
banknote-authentication	1097	275	4	0	2
bank-marketing	36168	9043	16	9	2
pc4	1166	292	37	0	2
kc2	417	105	21	0	2
diabetes	614	154	8	0	2

Table 4: Meta-testing datasets $\mathcal{D}_{\text{meta-test}}$. Train size is the number of training instances in d_{train} , and Test size is the number of test instances in d_{test} . Subscripts $i..j$ and (\cdot) denote the interval of indices and the total number of datasets of the same group used, respectively.

when selecting the optimal target model configuration for the task at hand by ensembling and fine-tuning the generated networks. In other words, the meta-model is fixed and ready to generate weights for a support set, without needing any hyperparameter tuning. For the fastest inference, predictions can be obtained by directly using the target network generated by HyperFast in a single forward pass. For slower but most accurate predictions, one can optimize the inference model configuration for each dataset by ensembling generated networks and fine-tuning them, using the recommended search space from Table 5.

Baselines Hyperparameter Selection For hyperparameter tuning of the baselines, we use Hyperopt (Bergstra et al. 2015), a Python library for hyperparameter optimization through Bayesian optimization. For XGBoost and CatBoost we adapt the hyperparameter search spaces from (Shwartz-Ziv and Armon 2022) and (Hollmann et al. 2023), which also tried other search spaces fixing the number of iterations and yielded suboptimal performance. For LightGBM we use the default hyperparameter search space defined in Hyperopt-sklearn (Komer, Bergstra, and Eliasmith 2014).

Parameter	Range
n_ensemble	[1, 4, 8, 16, 32]
batch_size	[1024, 2048]
nn_bias	[True, False]
optimization	[None, "optimize", "ensemble_optimize"]
optimize_steps	[1, 4, 8, 16, 32, 64, 128]
seed	[0, 1, ..., 9]

Table 5: Recommended search space for the inference framework of HyperFast.

For KNN and Logistic Regression we use the ranges used in (Hollmann et al. 2023), while for SAINT, the search space implemented in (Borisov et al. 2021). We benchmark DANet according to the configuration detailed in (Chen et al. 2022b), and for Net-DNF (Katzir, Elidan, and El-Yaniv 2020), we follow the search space suggested by the authors. For NODE (Popov, Morozov, and Babenko 2019), FT-Transformer (Gorishniy et al. 2021), and T2G-Former (Yan et al. 2023), we conducted experiments with the search

Model	Hyperparameter	Sampling	Range
KNN	n_neighbors	randint	[1, 16]
Log. Reg.	penalty	choice	[11, 12, none]
	max_iter	randint	[50, 500]
	fit_intercept	choice	[True, False]
	C	loguniform	$[e^{-5}, 5]$
XGBoost	learning_rate	loguniform	$[e^{-7}, 1]$
	max_depth	randint	[1, 10]
	subsample	uniform	[0.2, 1]
	colsample_bytree	uniform	[0.2, 1]
	colsample_bylevel	uniform	[0.2, 1]
	min_child_weight	loguniform	$[e^{-16}, e^5]$
	alpha	loguniform	$[e^{-16}, e^2]$
	lambda	loguniform	$[e^{-16}, e^2]$
	gamma	loguniform	$[e^{-16}, e^2]$
n_estimators	randint	[100, 4000]	
LightGBM	num_leaves	randint	[5, 50]
	max_depth	randint	[3, 20]
	learning_rate	loguniform	$[e^{-3}, 1]$
	n_estimators	randint	[50, 2000]
	min_child_weight	loguniform	$[e^{-5}, e^4]$
	subsample	uniform	[0.2, 0.8]
	colsample_bytree	uniform	[0.2, 0.8]
	reg_alpha	choice	[0, 0.1, 1, 2, 5, 7, 10, 50, 100]
	reg_lambda	choice	[0, 0.1, 1, 5, 10, 20, 50, 100]
CatBoost	learning_rate	loguniform	$[e^{-5}, 1]$
	random_strength	randint	[1, 20]
	l2_leaf_reg	loguniform	[1, 10]
	bagging_temperature	uniform	[0, 1]
	leaf_estimation_iterations	randint	[1, 20]
	iterations	randint	[100, 4000]
SAINT	dim	choice	[32, 64, 128, 256]
	depth	choice	[1, 2, 3, 6, 12]
	heads	choice	[2, 4, 8]
	dropout	choice	[0, 0.1, 0.2, 0.3, 0.4, 0.5, 0.6, 0.7, 0.8]
MLP	learning rate	loguniform	$[e^{-9}, e^{-3}]$
	batch size	uniform	[10, 2048]
	optimizer	choice	[Adam, AdamW, SGD, RMSprop]
	patience	uniform	[10, 50]
	validation split	uniform	[0.05, 0.5]
Net-DNF	number of formulas	choice	[64, 128, 256, 512, 1024, 2048, 3072]
	feature selection beta	choice	[1.6, 1.3, 1., 0.7, 0.4, 0.1]

Table 6: Hyperparameter search spaces for baseline methods. Hyperparameter configurations are drawn using the sampling technique specified in every range.

spaces provided in the original papers. However, the computational and runtime costs associated with these methods is very high, making it impractical to thoroughly explore the search spaces within the 48-hour limit set for the evaluation corpus. In every instance, configurations explored below this limit yielded inferior results compared to the default configuration of each method, with the default implementations,

surpassing the time limit on the big test. As an alternative to these challenges, we use the default configuration of the models on the mini test, and also perform a sweep of epochs until early stopping is performed (default case) to assess the improvement in performance within the runtime ranges of the models comparison. For the MLP, we replicate the exact same architecture as the main network produced by Hyper-

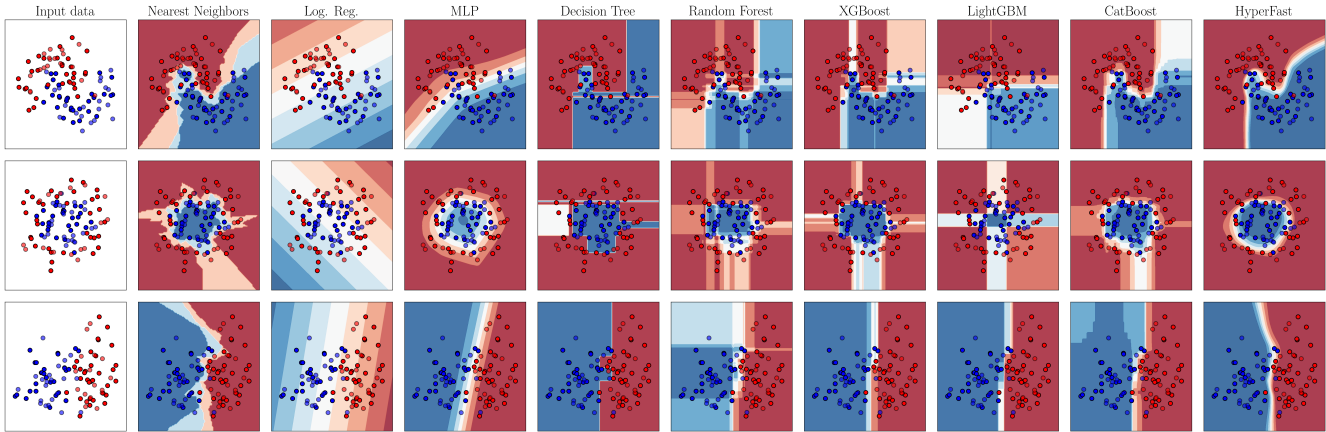


Figure 4: Classifiers comparison with the decision boundaries for toy binary classification datasets.

Fast, including the initial RF and PCA transformation layers. We perform hyperparameter tuning on the training hyperparameters, fixing the number of epochs to 1,000,000 and performing early stopping based on the validation loss. For TabPFN we consider up to 4096 data permutations for ensembling. Table 6 details the hyperparameter search spaces, as well as the sampling method used in every range for hyperparameter selection.

Additional Results

Toy datasets

In Figure 4 we compare HyperFast to traditional ML methods on toy datasets from scikit-learn (Pedregosa et al. 2011): *make_moons* in the top row, *make_circles* in the middle row, and a linearly separable dataset in the bottom row, all with Gaussian noise added. We can see how HyperFast models correctly the *moons* and *circles* without overfitting to the outliers, and creates a reasonably linear decision boundary for the bottom case. In contrast, tree-based methods overfit to the training data and fail to model accurately the distributions, creating abrupt and inaccurate decision boundaries in most cases.

How Can We Leverage All Labeled Data of a Large Dataset?

In a single forward pass, HyperFast can generate a set of weights for a smaller model ready for inference using a set of labeled samples. However, for datasets with large training sets it is not possible to use all available labeled data in a single forward pass due to memory and efficiency constraints, thus possibly losing relevant information from the dataset that could be valuable for the generation of weights to solve the task. We compare different options to leverage all labeled data in the generation of the final inference model in Figure 5.

We first experiment with increasing the batch size in a single forward pass. As we can expect, larger batch sizes yield significantly better performance, but at the cost of a much

slower runtime. This is mainly due to the singular value decomposition (SVD) performed in the PCA module, although implemented and optimized for GPU, the computation time scales rapidly with the number of input samples when an excessively large batch size is used. Thus, for the trained HyperFast and for the rest of experiments, we use a fixed maximum batch size of 2048 samples, which yields very good results in less than a second.

Multiple models can be generated from different subsets of datapoints, each capturing different variations between samples. Additionally, the random features projection matrix is reinitialized in every forward pass of HyperFast, injecting more variability in all the following generated layers across models, even if the same subset of samples is used in different forward passes. We combine the predictions of multiple generated models with soft-voting ensembles, and we observe that bigger ensembles make more accurate predictions. Another alternative we experiment with is stacking the predictions of multiple main models using a Logistic Regression as the meta-learner. However, performance stagnates and does not improve with more stacking members. We also try a variant of stacking, where instead of stacking predictions from multiple models and fitting a single meta-learner, we stack the predictions and all intermediate activations from a single model and fit a meta-learner. We repeat the process for several main models and meta-learners, creating an ensemble of meta-learners. Although it is a more expensive process, we find that it yields better results than traditional stacking, performing on par with ensembling but with higher runtimes. Furthermore, we consider the weights generated by HyperFast as an starting point for fine-tuning the model on all training data. Note that in this case, all model weights are optimized: random features, PCA parameters, and linear layer weights. In Figure 5 we see that optimizing the generated model in a single forward pass with all the training data, results are worse than ensembling for a small runtime budget. But for larger runtimes, optimization outperforms ensembling and stacking on their own. Finally, we combine the two fastest and best performing options, i.e., *Optimization + Ensembling*, where we generate models in

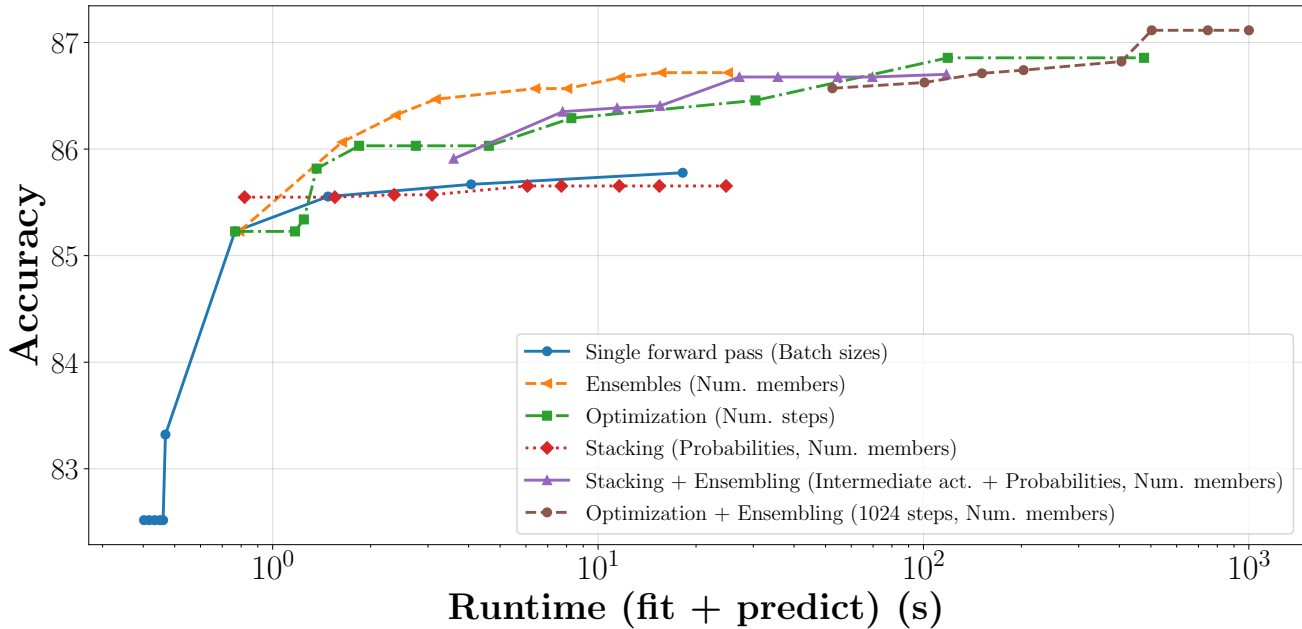


Figure 5: Performance as a function of runtime for different approaches to fully leverage all training data in the generation of the final inference model with HyperFast. Batch sizes considered in a single forward pass: [64, 128, 256, 512, 784, 1024, 2048, 4096, 8192, 16384]. Number of members considered in options involving ensembling or stacking: [1, 2, 3, 4, 8, 10, 15, 20, 32]. Optimization steps trials: [0, 2, 3, 4, 8, 16, 32, 64, 256, 1024, 4096].

	Log. Reg.	XGBoost	LightGBM	CatBoost	MLP*	ASKL 2.0	SAINT	DANet	Net-DNF	TabPFN	AutoGluon	HyperFast
hapmap ₁	47.899 ± 2.618	45.598 ± 2.412	46.037 ± 1.668	44.433 ± 1.555	46.870 ± 1.409	47.816 ± 1.928	39.750 ± 2.619	31.043 ± 8.923	39.288 ± 1.625	41.339 ± 1.942	47.992 ± 2.664	47.758 ± 1.437
hapmap ₂	49.675 ± 2.149	45.754 ± 2.242	47.502 ± 2.175	46.654 ± 1.709	48.564 ± 1.324	50.60 ± 1.924	40.534 ± 3.689	30.241 ± 5.934	39.776 ± 1.737	42.807 ± 1.650	49.598 ± 2.198	48.490 ± 1.736
hapmap ₃	49.702 ± 1.422	45.862 ± 2.421	47.613 ± 2.777	45.028 ± 2.389	48.221 ± 1.713	49.142 ± 2.082	38.380 ± 2.648	29.952 ± 8.464	38.917 ± 1.602	41.109 ± 2.151	48.920 ± 2.044	48.261 ± 2.020
hapmap ₄	50.331 ± 1.990	47.911 ± 2.854	46.988 ± 2.645	45.706 ± 3.018	48.473 ± 2.209	49.065 ± 2.190	40.792 ± 2.958	32.588 ± 6.857	39.580 ± 2.525	43.118 ± 1.945	50.077 ± 1.605	49.216 ± 2.082
hapmap ₅	50.221 ± 2.092	47.567 ± 3.638	48.385 ± 2.332	47.733 ± 2.917	49.761 ± 2.173	50.884 ± 3.262	41.271 ± 3.099	36.132 ± 7.936	39.925 ± 2.461	42.011 ± 3.045	50.668 ± 2.50	50.173 ± 2.156
phoneme	65.172 ± 3.023	80.824 ± 1.631	80.968 ± 1.513	81.926 ± 1.634	79.780 ± 1.331	81.831 ± 1.542	79.548 ± 1.154	75.092 ± 4.147	50.0 ± 0.0	81.080 ± 1.274	81.748 ± 1.128	80.794 ± 0.887
wilt	69.774 ± 7.629	85.155 ± 3.311	85.535 ± 2.320	85.957 ± 2.979	91.225 ± 2.727	88.956 ± 1.718	50.0 ± 0.0	50.0 ± 0.0	50.0 ± 0.0	91.420 ± 3.576	87.351 ± 3.730	89.054 ± 4.225
pendigits	92.974 ± 0.594	96.348 ± 0.847	96.805 ± 0.484	97.714 ± 0.385	97.936 ± 0.245	97.433 ± 0.447	77.179 ± 2.048	96.152 ± 2.768	80.425 ± 3.754	98.657 ± 0.241	97.783 ± 0.276	98.498 ± 0.378
satimage	79.126 ± 0.955	85.451 ± 1.025	85.654 ± 0.705	85.481 ± 0.748	85.372 ± 1.647	85.736 ± 0.949	84.739 ± 1.713	79.597 ± 8.511	79.048 ± 1.482	85.361 ± 1.066	85.984 ± 0.853	86.437 ± 0.542
credit-appr.	84.352 ± 0.0	87.290 ± 0.0	87.0 ± 0.082	84.352 ± 0.0	84.059 ± 0.850	84.257 ± 0.708	83.334 ± 0.891	80.892 ± 1.836	80.777 ± 1.264	80.594 ± 0.0	84.694 ± 0.987	80.594 ± 0.0
bank-auth.	98.693 ± 0.0	99.739 ± 0.138	99.837 ± 0.172	99.673 ± 0.0	100.0 ± 0.0	100.0 ± 0.0	100.0 ± 0.0	98.733 ± 1.519	93.727 ± 2.938	100.0 ± 0.0	100.0 ± 0.0	100.0 ± 0.0
bank-mkt.	65.952 ± 2.422	64.973 ± 2.773	64.507 ± 2.980	65.928 ± 2.215	59.738 ± 3.748	62.806 ± 5.105	57.260 ± 4.854	50.376 ± 1.180	51.802 ± 2.549	61.591 ± 2.699	61.054 ± 3.546	76.669 ± 1.330
pc4	68.351 ± 0.210	75.161 ± 1.205	74.963 ± 1.554	73.099 ± 1.918	71.497 ± 1.979	74.737 ± 3.870	66.743 ± 4.820	50.0 ± 0.0	59.314 ± 6.702	72.170 ± 1.249	71.359 ± 2.406	75.662 ± 2.736
kc2	65.170 ± 0.0	67.908 ± 0.0	67.442 ± 0.0	63.946 ± 1.761	66.265 ± 2.503	64.540 ± 0.758	65.115 ± 2.194	63.245 ± 5.950	50.0 ± 0.0	69.113 ± 0.0	62.878 ± 1.905	67.442 ± 0.0
diabetes	66.926 ± 0.0	72.204 ± 0.0	71.280 ± 0.327	69.630 ± 1.263	70.280 ± 1.161	67.593 ± 2.703	58.713 ± 3.241	63.261 ± 5.322	58.565 ± 6.963	68.778 ± 0.0	68.935 ± 1.431	70.907 ± 0.0
Mean rank	5.953 ± 0.191	4.747 ± 0.514	4.660 ± 0.488	5.347 ± 0.514	4.720 ± 0.478	4.30 ± 0.542	8.533 ± 0.439	9.373 ± 0.524	10.113 ± 0.252	6.093 ± 0.308	4.273 ± 0.341	3.547 ± 0.408
Mean bal. acc.	66.955 ± 0.525	69.850 ± 0.316	70.034 ± 0.461	69.151 ± 0.328	69.869 ± 0.372	70.360 ± 0.492	61.557 ± 0.647	57.820 ± 1.470	56.743 ± 0.827	67.943 ± 0.435	69.936 ± 0.455	71.330 ± 0.445

Table 7: Balanced accuracy results per dataset on the mini test for a runtime budget of 5 minutes. The mean rank of each method is also shown, for 10 repetitions with different selection of samples and features to subset and create the mini test. MLP*: MLP with the exact same architecture as the main network produced by HyperFast, including the initial RF and PCA transformation layers.

different forward passes, optimize them, and combine the fine-tuned models by ensembling. We perform 1024 fine-tuning steps in each generated network with a batch size of 2048, using the AdamW optimizer with a learning rate of $1e-4$, and a scheduler that reduces the learning rate by a factor of 0.1 when the loss stagnates for 10 steps. We observe that although this combination requires more runtime, a single fine-tuned model matches the performance of large ensembles of non-optimized models, and a large ensemble of fine-tuned models yields the best results. We show results by starting with a single forward pass, then increasing the ensemble size by performing multiple forward passes until GPU memory is overloaded. Then, we restart the sweep by

optimizing each generated model and ensembling the fine-tuned networks.

Extended Results of Experiments

Extending the results of the main paper, Table 7 shows per dataset results on the mini test, for a total runtime budget of 5 minutes, and 10 repetitions for different sample and feature subseting to create the small-sized mini test. These results show that HyperFast is the best option for a rapid deployment setting, outperforming TabPFN, AutoML systems and other methods. Additionally, Table 8 shows the results on the mini test for a 1h budget, but we allow an extended total runtime of 48h on the 15 datasets. With a sufficient amount

	LR	XGB	LGBM	CatB	MLP*	ASKL2	SAINT	DANet	Net-DNF	NODE	TabPFN	FT-T	T2G	AG	HF
hapmap ₁	48.195	45.353	46.649	47.209	47.490	45.278	47.049	19.868	43.832	43.303	41.262	44.304	43.787	47.769	49.640
hapmap ₂	51.434	51.372	47.968	48.139	51.529	49.552	49.332	27.122	48.572	49.535	42.778	50.242	48.085	51.741	51.197
hapmap ₃	50.294	47.162	48.821	44.927	48.348	50.087	50.384	28.614	44.549	47.806	40.464	49.230	47.070	49.511	49.701
hapmap ₄	51.347	49.222	50.676	47.784	49.808	51.299	46.988	31.779	44.880	45.332	40.572	45.256	47.604	53.314	49.640
hapmap ₅	52.170	52.122	50.934	51.282	52.133	49.512	50.058	28.311	47.017	46.791	41.189	48.647	47.195	51.131	51.190
phoneme	66.526	82.420	81.685	83.601	82.035	83.769	80.716	70.754	50.0	80.403	80.703	82.953	81.691	82.970	81.146
wilt	77.284	89.259	90.003	90.166	91.019	91.073	50.0	50.0	50.0	50.0	88.352	92.833	95.587	90.964	91.073
pendigits	93.944	97.038	97.155	98.085	97.978	98.062	76.753	97.897	90.571	96.250	98.823	97.486	97.541	98.291	98.652
satimage	80.791	86.493	86.721	86.857	86.317	87.155	86.420	84.769	83.480	87.016	87.358	86.073	86.274	87.074	87.416
credit-appr.	84.352	86.30	87.119	86.30	85.650	85.480	84.831	78.720	83.532	84.288	81.893	86.438	86.268	85.650	82.063
bank.-auth.	98.693	100.0	100.0	99.673	100.0	100.0	100.0	98.854	99.673	100.0	100.0	100.0	100.0	100.0	100.0
bank.-mkt.	70.475	69.063	67.949	70.859	70.508	62.490	61.104	56.968	54.101	64.596	65.0	70.648	64.214	65.529	75.656
pc4	68.663	78.798	77.604	76.411	76.432	83.181	72.873	49.609	61.914	66.102	74.631	70.877	66.710	73.438	78.212
kc2	65.170	64.567	67.442	64.567	69.113	67.908	66.840	61.829	65.772	65.170	69.715	69.113	66.375	65.635	72.453
diabetes	67.0	75.759	71.130	71.981	71.981	76.889	63.444	67.074	71.278	68.352	70.204	68.074	64.944	70.556	70.907
Mean rank	7.467	5.933	6.20	5.667	4.533	4.533	8.60	12.467	11.067	9.733	8.80	6.667	8.667	4.60	3.933
Mean bal. acc.	68.423	71.662	71.457	71.189	72.023	72.116	65.786	56.811	62.611	66.330	68.196	70.812	69.556	71.572	72.596

Table 8: Balanced accuracy results per dataset on the mini test with extended runtime. The mean rank of each method is also shown. LR: Logistic Regression; XGB: XGBoost; LGBM: LightGBM; CatB: CatBoost; MLP*: MLP with the exact same architecture as the main network produced by HyperFast, including the initial RF and PCA transformation layers; ASKL2: ASKL 2.0; FT-T: FT-Transformer; T2G: T2G-Former; AG: AutoGluon; HF: HyperFast.

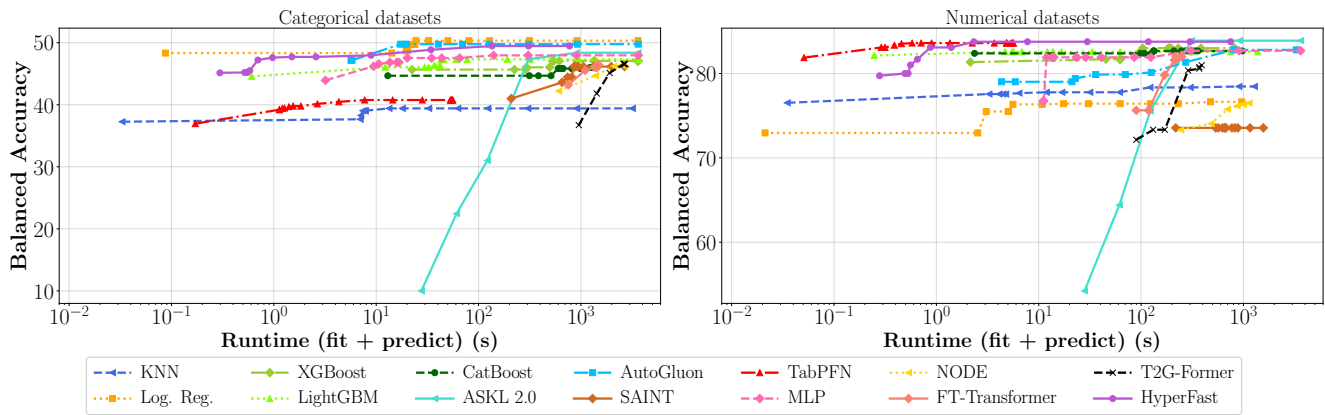


Figure 6: (left) Categorical datasets of the mini test. (right) Numerical datasets of the mini test.

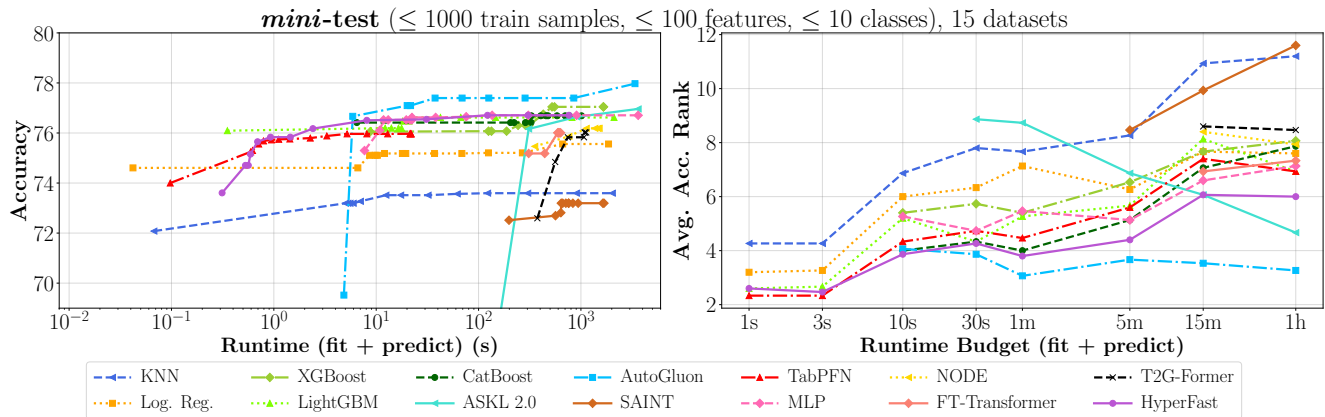


Figure 7: Runtime (fit + predict) vs. regular accuracy and average rank for given runtime budgets on the mini test: 15 small-sized meta-datasets.

	LR	XGB	LGBM	CatB	MLP*	ASKL2	SAINT	DANet	Net-DNF	AG	HF
hapmap ₁	74.299	71.396	70.750	68.608	74.169	76.397	61.874	16.029	58.501	76.712	80.497
hapmap ₂	73.507	63.447	70.622	70.695	73.509	75.869	62.326	29.873	63.359	77.210	78.693
hapmap ₃	76.007	66.742	71.436	72.079	75.949	78.481	60.510	65.724	62.977	79.548	78.828
hapmap ₄	75.60	74.043	71.346	68.860	75.275	77.388	52.228	66.506	62.718	79.894	81.782
hapmap ₅	79.435	67.059	72.009	72.045	80.106	80.797	61.833	32.847	64.505	82.374	83.364
phoneme	64.553	84.717	86.633	85.467	83.482	87.975	81.384	70.323	81.116	86.422	83.863
wilt	69.974	89.150	88.189	91.019	91.980	93.958	50.0	50.0	69.231	93.051	93.903
pendigits	94.737	98.998	99.184	99.275	99.596	99.232	94.622	98.721	91.945	99.505	99.501
satimage	81.057	89.390	89.824	89.708	89.157	89.655	86.325	89.319	82.235	90.942	90.813
credit-appr.	84.352	86.949	87.119	86.30	84.490	84.831	81.105	80.424	81.754	85.480	82.063
bank.-auth.	98.693	99.673	100.0	99.673	100.0	100.0	99.673	99.673	93.453	100.0	100.0
bank-mkt.	66.174	71.593	73.814	73.771	72.952	75.426	71.687	65.436	66.523	71.491	77.019
pc4	68.273	75.022	76.606	76.606	74.240	82.986	55.360	50.0	66.688	72.049	80.599
kc2	65.170	61.090	68.045	64.567	71.249	67.908	67.908	67.442	50.0	63.499	72.453
diabetes	67.0	72.056	71.130	71.981	72.407	74.185	50.0	65.426	67.352	69.852	73.185
Mean rank	6.867	5.867	4.667	5.0	4.333	2.733	8.667	9.0	9.0	3.467	2.267
Mean bal. acc.	75.922	78.088	79.780	79.377	81.237	83.006	69.122	63.183	70.824	81.868	83.771

Table 9: Balanced accuracy results per dataset on the big test with extended runtime. The mean rank of each method is also shown. LR: Logistic Regression; XGB: XGBoost; LGBM: LightGBM; CatB: CatBoost; MLP*: MLP with the exact same architecture as the main network produced by HyperFast, including the initial RF and PCA transformation layers; ASKL2.0; AG: AutoGluon; HF: HyperFast.

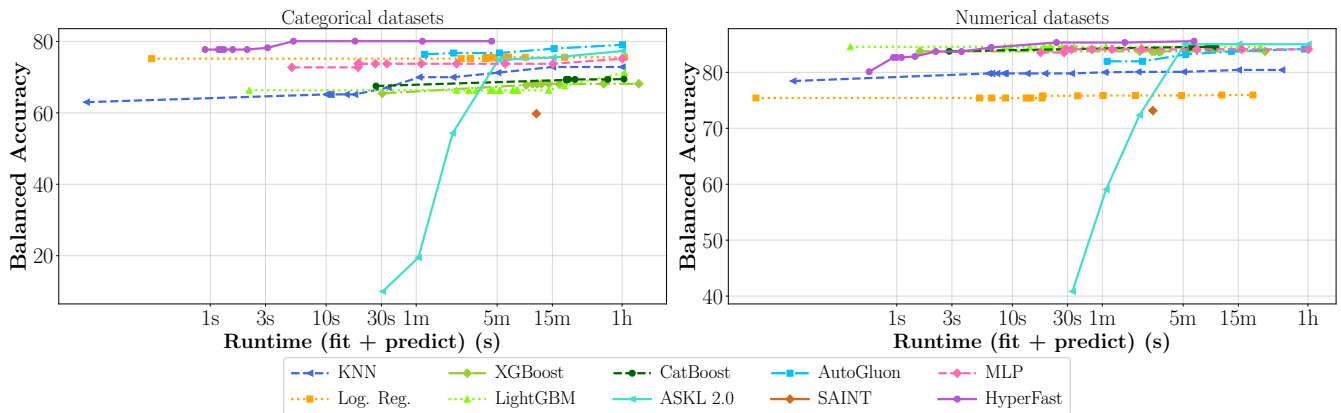


Figure 8: (left) Categorical datasets of the big test. (right) Numerical datasets of the big test.

of time for hyperparameter tuning on such small datasets, HyperFast is the best overall performing method, followed by AutoML systems and the MLP matching the architecture of HyperFast’s generated main network, including the RF+PCA initial layers. In Figure 6 we can see that TabPFN underperforms for categorical datasets but obtains competitive performance for numerical datasets in a very low runtime. However, it is outperformed by HyperFast with a runtime of 2 seconds. Figure 7 shows the mini-test results in terms of regular accuracy, where TabPFN surpasses HyperFast for low runtimes, and AutoGluon also obtains better accuracy for high runtimes. This is contrary to the balanced accuracy results, which indicates that these models may underperform in accurately predicting minority classes on imbalanced datasets.

For the large datasets setting, Figure 8 shows the results of the different classifiers separated for fully categorical and numerical datasets. HyperFast obtains the best balanced accuracy results across all runtime regimes for categorical datasets. In contrast, gradient-boosting machines obtain better results for small time budgets on numerical datasets, but AutoML systems and HyperFast rapidly match and surpass their performance when more time is given to create larger ensembles and fine-tune each member. We show detailed results per dataset in Table 9 for the big test on a 1h budget per dataset, with a total extended runtime limit of 48h. In a large-scale setting, tree-based gradient-boosting machines and the MLP are outperformed by AutoML systems which, in fact, train multiple instances of these gradient boosting algorithms and neural networks (among other models) to build

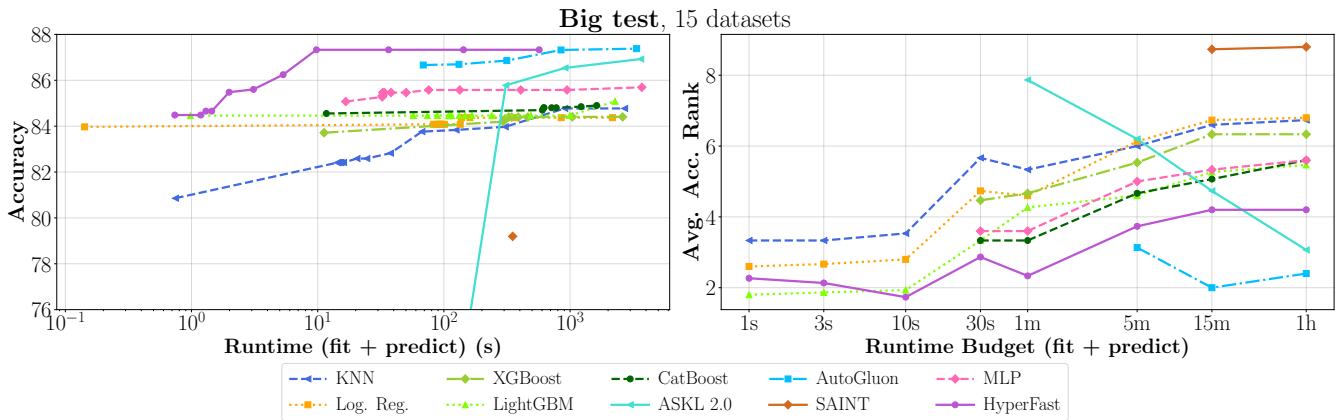


Figure 9: Runtime (fit + predict) vs. regular accuracy and average rank for given runtime budgets on the big test: 15 large/medium-sized meta-datasets.

a stronger predictor. The resulting ensemble is increasingly powerful when long fitting time budgets are allowed. Figure 9 shows that HyperFast is outperformed by AutoML systems for long runtimes in terms of regular accuracy. However, HyperFast obtains the best balanced accuracy results, which suggests that HyperFast is the model that performs more consistently across different classes, particularly in datasets where some classes are underrepresented.

When it comes to individual datasets, HyperFast outperforms other methods, especially in fully categorical datasets. One reason is the use of PCA projections before the neural layers, and the concatenation of the global average and per class average of the PCA projections to each hypernetwork module. Previous work on genetic datasets (Novembre et al. 2008) demonstrated the capability of PCA-based methods to capture the variation of samples and structure of the data. In the case of more diverse tabular datasets that have no underlying structure, the use of PCA does not have a negative impact. As a result, we have observed HyperFast also outperforming other baselines in diverse OpenML tabular datasets. When using a large number of principal components (PCs) (784) there is no information loss for datasets with d features if $d \leq 784$, which is the case for most datasets considered. Information loss in datasets with $d > 784$ is minimal, since we keep the first 784 PCs associated with the largest eigenvalues, while the remaining components explain the least amount of variance in the data. The ablation studies show that even decreasing the number of PCs to 512, performance is not very affected, while removing the PCA transformation results in the largest drop in performance. The volume of support samples also has an effect on HyperFast’s performance, as larger datasets provide more robust statistical basis for the hypernetwork to accurately predict weights. In contrast, a limited number of support samples may restrict the hypernetwork’s ability to capture the statistical properties of the dataset, consequently affecting the accuracy of the generated main network.

High-Dimensional Biomedical Datasets

In real-world biomedical applications, many tabular datasets exhibit very high dimensionality, making gradient-boosted trees computationally expensive and prone to overfitting, while traditional linear methods fail to capture non-linear interactions, leading to suboptimal modeling performance. Additionally, current deep learning methods can struggle with scalability and present unfeasible training challenges when applied to datasets of such scale.

A meta-trained and scalable model, such as HyperFast, offers a new approach to address these issues and provides an alternative classification approach for real-world applications. In this work, we conduct additional experiments on two high-dimensional biomedical datasets. First, we use *hapmap-100k*, a HapMap3 (Consortium et al. 2010) dataset following the steps described in the Experimental Setup, but randomly selecting a total of 100,000 SNPs from all the available SNPs without missing data. Next, we utilize *diabetes-31k*, a UK Biobank diabetes prediction dataset including underrepresented populations (Bonet et al. 2024). While such biobanks include more diverse genetic backgrounds, the majority group in the UK Biobank includes individuals with European (British) ancestry, and other groups are still highly underrepresented. This dataset includes 31,153 SNPs for 66,302 individuals with European, South Asian, African, and East Asian ancestry.

Model	hapmap-100k	diabetes-31k	
		All	Underrep. only
Lasso	93.564	54.365	53.376
Elastic Net	94.208	53.454	52.708
LightGBM	83.301	50.412	50.419
XGBoost	82.475	50.561	50.351
HyperFast	95.889	64.327	54.023

Table 10: Balanced accuracy on high-dimensional biomedical datasets.

In the case of high-dimensional datasets where the support set including all features does not fit in GPU memory, we adapt HyperFast to perform feature bagging. For these experiments, we create ensembles of 32 networks and perform fine-tuning. For each ensemble member, HyperFast samples a subset of 3,000 SNPs from a multinomial distribution weighted by their standard deviation.

The results in Table 10 highlight HyperFast’s robustness in high dimensional settings, achieving the best performance in both biomedical datasets, followed by the linear models. Remarkably, HyperFast obtains a 10% increase in balanced accuracy in *diabetes-31k* for test samples of all populations, and also obtains stronger predictions when only analyzing the performance for test individuals that are under-represented in the training data.

Limitations

In terms of number of samples, HyperFast takes a fixed number of training samples (support set) to predict a single set of weights. For very large datasets, the generated main network in a single forward pass will not deliver optimal results, as the sample of data points used for the generation might not fully represent the entire dataset distribution. However, rapid improvements can be obtained with the optimization and ensembling techniques detailed previously, enabling the use of any dataset size. Regarding the number of features, the input size is not fixed, as HyperFast projects the original data of any given feature size with the random features and PCA module to a fixed size. In a single forward pass, the number of input features is only restricted by the amount of GPU memory available. To address this issue, feature bagging can be used together with ensembling for dealing with very high-dimensional datasets. Note that if the number of selected features for an ensemble member is much larger than the number of PCs used, some information might be lost. To address this, one can train larger versions of HyperFast by increasing the number of retained PCs.

Our work prioritizes a simple yet effective method suitable for most tabular datasets within a constrained computational environment. Future work could explore expanding HyperFast to regression tasks and transitioning to a large-scale setup utilizing multiple GPUs for the meta-training of the model, where most information could be retained for very large numbers of features or different modalities (e.g., high resolution images). We also leave as future work the study of dataset distribution differences from meta-training and how it affects generalization performance. Lastly, in terms of number of categories, the HyperFast version discussed in this paper supports up to 100 classes. Nonetheless, training a HyperFast to accommodate more categories would increase linearly the complexity of the initial layers of the hypernetwork modules, which accounts for very small memory and computational requirements.